Scholars' Mine

Spring 2015

Spatial and temporal modulation of heat source using light modulator for advanced thermography

Arvindvivek Ravichandran

SPATIAL AND TEMPORAL MODULATION OF HEAT SOURCE USING LIGHT

MODULATOR FOR ADVANCED THERMOGRAPHY

by

ARVINDVIVEK RAVICHANDRAN

A THESIS

Presented to the Faculty of the Graduate School of the

MISSOURI UNIVERSITY OF SCIENCE AND TECHNOLOGY

In Partial Fulfillment of the Requirements for the Degree

MASTER OF SCIENCE IN MECHANICAL ENGINEERING

2015

Approved by

Edward Kinzel, Advisor
Xiaodong Yang
Hai-Lung Tsai

ABSTRACT

Thermography is a Non-Destructive Testing (NDT) method that has found increasing use in industry and research. It has the advantages of being non-contact and be able to interrogate a large surface simultaneously. Active thermography using flash lamps as heat source has been demonstrated for identifying blind holes and delamination in composites. Despite these advancements, active thermographic approach fails to defects like cracks. Under uniform illumination heat flow is predominantly 1D and can easily circumvent a narrow feature. This can be overcome by using a focused light/laser source onto the surface to impose a 3D heat flux. The disadvantage is that thermography is now a point-by-point proposition, because the focused heat source interrogates only a localized region. This work investigates the use of a Digital Micro mirror Device (DMD) to modulate the illumination both spatially and temporally. This allows multiple point or line sources to simultaneously illuminate a surface at independent frequencies. The use of frequency modulation maps the results to phase space, which permits data to be extracted even when the thermal camera is not precisely calibrated, in combination with the low cost of the DMDs. This thesis describes the construction of the experiment, the theory behind the technique, demonstrates the setup for conventional thermographic methods (pulse/flash and lock-in) before demonstrating the ability to demodulate a locally varying heat flux. The thesis also presents the use of the setup for rudimentary system identification which is similar to Photo Thermal Radiometry, and extends the use of the setup to distinguish films from the underlying substrate, in addition to crack detection. Numeric simulations in ANSYS used to guide this work are also presented along with suggestions for future improvement of the setup and scale-up to larger systems.

ACKNOWLEDGMENTS

TABLE OF CONTENTS

LIST OF ILLUSTRATIONS

LIST OF TABLES

NOMENCLATURE

Symbol	Description
Q	Heat Flux in W/m^2
T	Temperature in ˚C
c_p	Specific Heat in J/kg. K
φ	Phase in Radian
ρ	Density in kg/m^3
ε	Radiation Emissivity
ω	Angular Frequency in rad/s
f	Frequency in Hz
z	Thermal Penetration Depth
k	Thermal Conductivity in W/mk
α	Thermal Diffusivity in m^2/s
t	Time in Seconds

1. INTRODUCTION

In today's manufacturing Industry the goal is to march towards excellence with zero tolerance in defects. The goal seems unrealistic due to the volume of products that are manufactured for the ever increase in the consumers. To touch the unrealistic goal, companies started implementing systematic quality improvement tools like sig sigma, lean, kaizen etc. In order to measure their progress, they rely on statistical methods which compute the estimate of quality with certain confidence intervals by random sampling of lot. The computed value is still an estimate and is not exact. Hence, the future is to ensure the quality of all the products that are manufactured by nondestructive methods using autonomous systems. This is enabled with the advanced tools developed under the science of Non-Destructive Testing [NDT]. NDT is not only important for ensuring the quality of the products during manufacturing process but also for verifying the quality during service hours. It is highly important in aerospace industry where the quality of the aircraft should be monitored before every flight in order to make sure there is zero percent failure [1, 2]

1.1 NON-DESTRUCTIVE TESTING

Non-Destructive Testing is a self-explanatory word describing the ability to identify discontinuities or defects without dissecting apart the component under study. This science of Non-Destructive Testing is very old. The early chronological events are described in the handbook of nondestructive evaluation[3].

NDT has several advantages compared to its peers. Some of the key features are (i) NDT is highly useful because of its capability to be deployed at larger scale. NDT can inspect the defects in the entire batch under production rather than testing random samples in batch. This brings more confidence in the quality of the product. (ii) The sample under study can be inspected even when it is performing its functionality (iii) The testing is simple and cost effective in most of the cases. (iv) The sample is not damaged or influenced under by the NDT when chosen aptly.

It has a wide variety of applications and is applied in diverse industries like aviation[1, 2, 4, 5], semiconductor[6-8] , manufacturing [9, 10], military[11, 12] , automotive [9, 13, 14]etc.

Out of the several applications, the most common defects are used to evaluate the structural defects like cracks, delamination, blow holes or voids in solid material.

There are several NDT methods like visual inspection, penetrant testing, magnetic particle testing, radiographic testing, ultrasonic testing, eddy current testing, thermal imaging, acoustic emission testing. Out of the several NDT techniques, thermography is one of the robust, inexpensive, non-contact techniques practiced by the industry.

1.2 NDT-THERMOGRAPHY

Thermography is one of the commercial NDT techniques. It is popular because of its remote inspection mechanism. The other competitive techniques require contact probes or signal sources placed over the surface. In Thermography both the signal source and the detector are placed in remote location from the object under inspection.

The key science behind thermography is Plank's law which describes the electromagnetic radiation emitted by a blackbody at definite temperature which is in thermal equilibrium. It is described using Equation.1. The first and second radiation constant are $C_1 = 3.742 \text{ X } 10^8 \text{ W}.\mu m^4 / m^2$ and $C_2 = 1.439 \text{ X } 10^4$ μm.k . By knowing the electromagnetic radiation intensity, the temperature of the surface of the blackbody can be determined. This principle is used in thermal camera which is basically an energy meter tuned to the spectral bandwidth of interest. By calibration, the exact temperature of the surface is determined.

$$E_{\lambda,b}(\lambda,T) = \frac{C_1}{\lambda^5[\exp(C_2 / \lambda T) - 1]}$$
(1)

The heat propagation through the defect is hindered and the energy gets accumulated. This accumulated energy rises the temperature of the material. This temperature rise at the surface of the material is proportional to the radiation emitted. This emitted radiation is detected through the FPA detector in the thermal camera. Thus a contrast in temperature profile is used to find the defect.

When identifying the defect there are three main requirements in NDT thermography. They are (i) Locating the defect (ii) Characterizing the profile of the defect (iii) Characterizing the material causing the defect. The priority of interest is in the descending order. Predominantly the later part is ignored due to complexity of the procedures involved.

The location of the defect is a qualitative measurement than quantitative. Compared to locating the defect, characterizing the depth and the size of the defect is a quantitative measurement. Then, characterizing the material inside the defect is even more quantitative.

Broadly Thermography is classified as active and passive thermography based on the heat source. Passive thermography is monitoring a sample using IR-camera without applying any heat over the sample. This is a very primitive technique where the defects are visible due to discontinuity of the heat. The drawback is that, the contrast is very minimal and there is no control over the resolution. So, in this work only active thermography is discussed.

The typical active thermography set up is shown in Figure.1. When the surface is heated with the heat source the heat propagation within the material is observed through the Infra-red camera. The heat source depends on the nature of the material, as different materials have different capability to absorb, transmit and reflect the electromagnetic radiation. They are usually denoted by the corresponding co-efficient of absorptance, transmittance and reflectance.
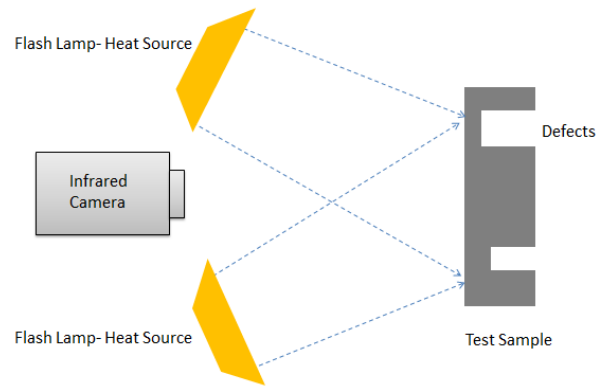
Figure.1.1 Typical Thermography set up of the sample and the IR camera

Active thermography can be broadly classified as (i) Pulse Thermography and (ii) Lock-in Thermography. They are discussed below:

1.1.1. Pulsed Thermography. In Pulsed thermography [2, 3, 5, 15-17], the sample to be inspected is heated on the surface by a heat source and is visualized by the detector. Usually, the heat source is a flash lamp or Laser beam and the detector is an IR Camera/detector.

Simple Pulse thermography set up is shown in the Figure.2.The source is a halogen flash lamp which is switched ON and OFF for short period of time. The source emits a short pulse of thermal energy Q over the surface.
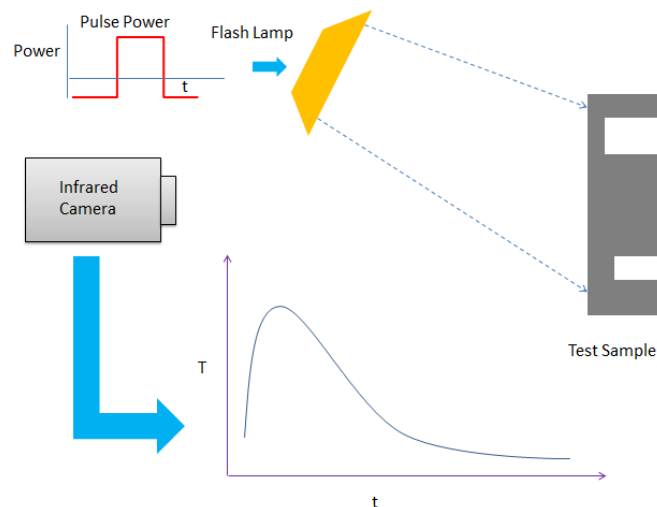
Figure.1.2 Experimental Set-Up of the Pulse Thermography

The governing equation is given by Equation (2), assuming that the body is semi-infinite where z the depth from the surface is Infinite. Effusivity of the body over the time period t is defined by e.

$$T(z = 0, t) = \frac{Q}{e\sqrt{\pi t}} \tag{2}$$

In the Figure.1.2, the surface temperature rise is plotted over time t at a specific location. Each specific location yields a temperature time history. There is a difference between the sample location without the defect and with defect. This is shown in qualitative seen in the Figure.1.3. The thermograph will show uniform heat propagation over the surface at T =0 when the sample doesn't have a defect. The thermograph will show the development of hot spot when there is a defect in the sample. This defect is in fact creating a resistance to the thermal wave propagation and there is an accumulation of thermal energy. This usually, is seen as a hot spot which is contrasting from the background. The thermal contrast is given by the Equation (3) where t' is the time when no defect is found. $T_d(t)$ is the temperature at the defect at time t.

$$\delta T = T_d(t) - \sqrt{\frac{t'}{t}} T(t') \tag{3}$$
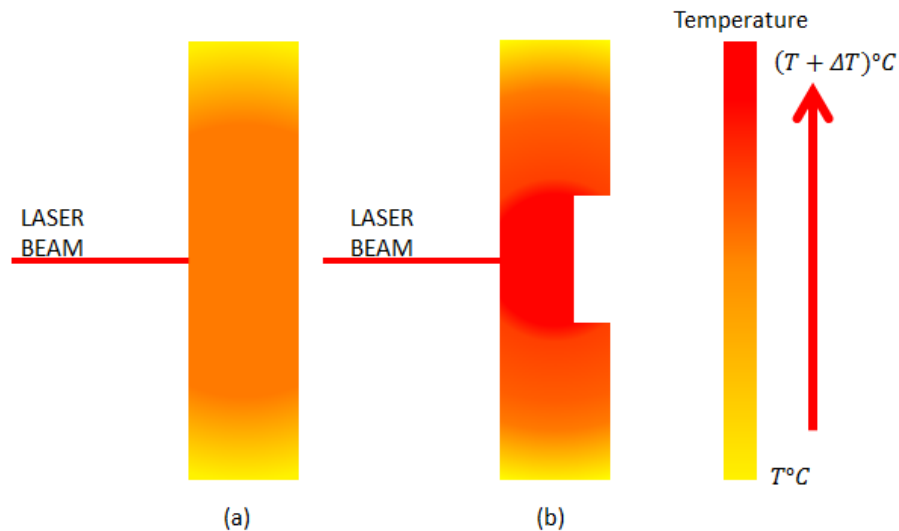
Figure.1.3 2-D Side View of Sample (a) Without Defect (b) With Defect with Pulse Thermography

Typical time history plot obtained from the thermograms over the time domain is shown in   Figure.1.4.
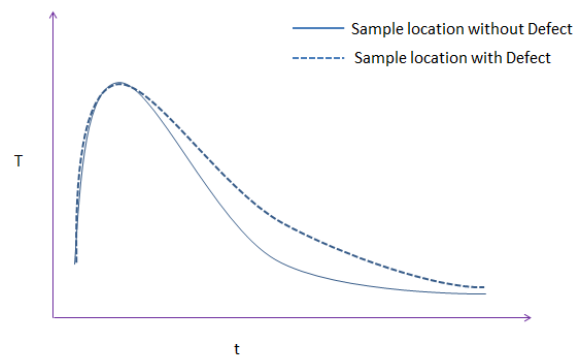
Figure.1.4 Plot showing the temperature profile of the pixels at locations without and with defects

The time domain curves at locations with and without the defect are plotted . From the difference in the rate of change of the curve, the defect can be estimated. The key drawback of this method is the prior information on time history of heat propagation on good sample in order to identify it from the defects. Also the background noise is not filtered in this method which can yield to wrong interpretation. Lock-in thermography is used to avoid these shortcomings, which is discussed in the next section.

1.1.2 Lock-In Thermography. Lock-in thermography is yet another active thermography which is widely used to identify the defects precisely in composites, stainless steel, etc. [6, 18-22]. In this technique the source is a periodic heating element. Usually, it is a Halogen lamp or a Laser depending on the sample under investigation and the amount of heat required.
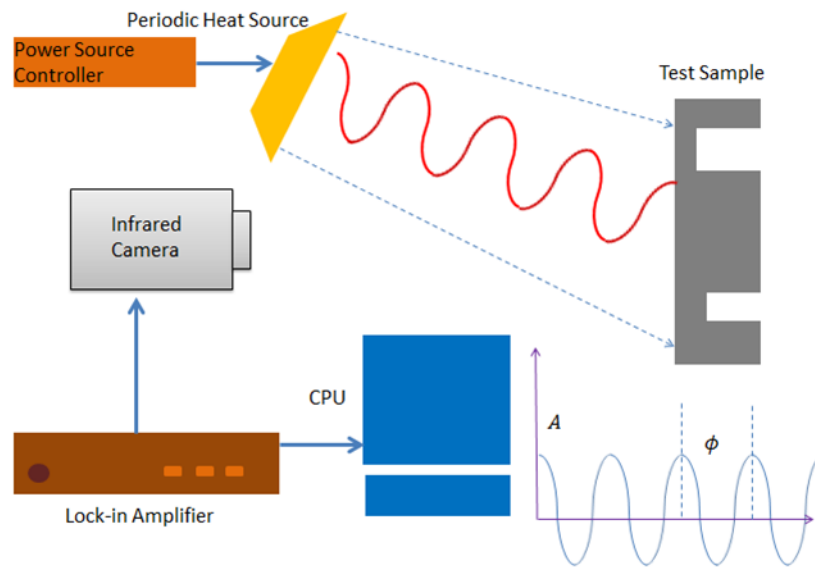
Figure.1.5 Conventional experimental set up of the Lock-in thermography

A simple Lock-in Thermography set up is shown in Figure.1.5. The periodic heating of the surface is captured through the IR camera. The signal from the camera is locked in to the frequency of the source. This enables to filter the noise and see the periodic variation corresponding to the source frequency. From the signal, by performing a Fast Fourier Transform the amplitude A and phase ϕ of the signal is identified and mapped out for each pixel.

From the heat transfer perspective, the physics is explained briefly as below. The fundamental math of the periodic heat source is given by the Equation (4), which is introduced by Carslaw.H.S[23].The heat propagation is governed by the heat equation shown in Equation (4). Heat equation explains the thermal diffusivity α .On applying the

boundary condition for semi-infinite medium and defining the surface temperature in terms of periodic variation described by Equation(5) on Equation(4), the solution is as described in Equation(6).

$$\frac{\partial T}{\partial t} = \alpha \nabla^2 T \tag{4}$$

$$T(0,t) = Ti + \Delta T \sin(\omega t) \tag{5}$$

$$\frac{T(x,t) - Ti}{\Delta T} = e^{(-x\sqrt{\omega/2\alpha})} Sin(\omega t - x\sqrt{\omega/2\alpha}) \tag{6}$$

This technique is the state of art in identifying the defects in the materials using thermography. The key disadvantage is that, this method uses sophisticated equipment which prevents the usage for most common purposes. The usage of Acoustic Opto Modulator (AOM) and lock in amplifier not only increases the complexity of the system, but also increases the cost of deployability.

Thus, this system is not suitable for extensive mobile applications.

1.3 SPATIAL TEMPORAL MODULATION TECHNIQUE

In this advanced photo thermal technique, the robustness is accomplished with light modulator which can modulate the heat source spatially and temporally, thereby reducing the cost of signal controller and spatial modulator. Add on to that, cheap un-calibrated, uncooled micro bolometers are used as the results are just sensitive to phase.

The simplified experimental setup is described in a 3D Block diagram and is shown in Figure.1.6. The heat source from diode laser shines the laser beam over the DMD (Digital Micro mirror Device). The output of the diode laser is streamlined through an optic fiber which is collimated over the DMD module of the Projector assembly. The micro mirrors in the DMD are controlled via MATLAB through a video output from the CPU.

The beam that is reflected and diffracted from the micro mirror is converged to form an image with the help of a convex lens. The beam is collimated over the sample. The

sample is said to be semi-infinite when the thickness of the sample is more than 5 times the thermal penetration depth. The thermal penetration depth or the thermal diffusion length is the length of the sample till which the heat wave reaches for a particular lock-in frequency. It is usually denoted by 'z'. It is a function of Thermal diffusivity, α and Lock-in frequency, f. It is given by Equation (7),

$$z = \sqrt{\frac{\alpha}{\pi f}} \tag{7}$$

The image acquired from the thermal camera is processed through MATLAB. The Fast –Fourier transform is performed to attain amplitude and phase information at the lock in frequency. The slope of the phase map for a given material gives a relation between the thermal properties of the material. Thus, the material can be identified in a remote fashion. The DMD helps in performing similar to localized photo thermal radiometry technique. With this multiple capabilities mobile system identification is possible.
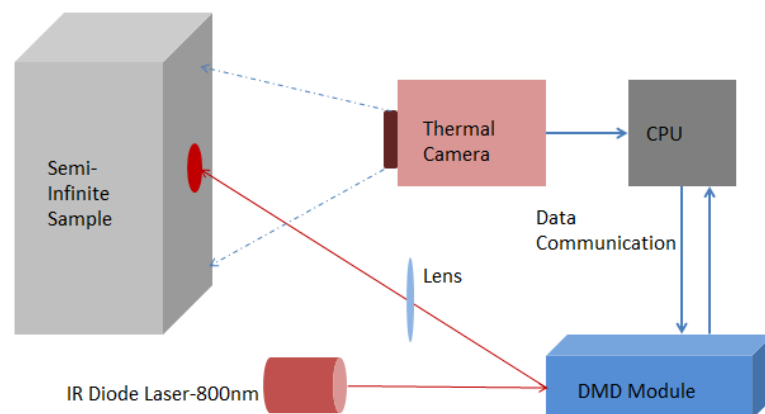
Figure.1.6 3-D Block Diagram representing the simplified experimental set-up
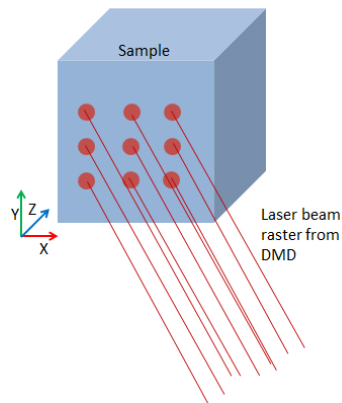
Figure.1.7 The laser beam raster and pulse over the surface as per the desired frequency

Thus this technique brings the best of both the world of NDT-Thermography and Photo thermal radiometry.

1.4 MOTIVATION

There is a need to develop a system which can identify the defects and discontinuities which are fine cracks both qualitatively and quantitatively in a remote, non-destructive fashion in diverse fields like Military, Aerospace Industry, and Electronics Industry etc. The qualitative method is applied in robust testing of surface defects. Also there is a need to perform system identification based on thermal properties which is robust and compact. The combination of spatial and temporal modulation of point and line heat source helps in identifying the cracks. When this modulation is performed similar to photo thermal radiometry the thermal diffusivity can be estimated. From the slope of the phase roll the thermal diffusivity could be approximated there by predicting or distinguishing between conductive and nonconductive surfaces.

In this work, the cost is limited due to elimination of multiple laser sources and complex instrumentation like Acoustic Opto Modulator (AOM) and Lock-in Amplifier. And more novelty is added by the use of Digital Micro-mirror Device (DMD) for spatial temporal modulation of multiple heat sources at different frequencies. The whole instrument is made cheap and robust with the help of uncooled micro bolometer which weighs less than 30g.

1.5 THESIS OVERVIEW

In this thesis, the experimental design and demonstration of cost effective instrument to perform spatial temporal modulation for advance thermography apart from conventional thermography is discussed. Under advance thermography, the capability of the instrument to identify surface cracks and capability to spatially modulate multiple heat sources are discussed. Apart from thermography, principles of radiometry are also demonstrated for system identification. Under system identification, distinguishing the materials based on the thermal diffusivity is demonstrated and discussed.

The thesis is sliced into five major segments, namely, the Introduction, DMD device and its architecture theoretical background and Numerical analysis, Thermal property estimation, results with discussion and finally the conclusion with future scope of the work.

In the first chapter the conventional thermography and spatial temporal modulation thermography is discussed describing the fundamentals and scope of each technique. Then, The need for this work and how it could lead to commercially used is explained. In the second chapter, the DMD device along with its architecture is described. Then, in the third chapter, the numerical analysis of 2-D models is described along with the governing equation for pulse, lock-in thermography, the boundary conditions and the procedure in making a numerical analysis using ANSYS Workbench is described. The numerical work helps in understanding the physics of the problem and possible solution. In the fourth chapter, the principles of photo radiometry along with the theory and application are discussed. In chapter five, the results of all the experiments and numerical simulation are discussed. The demonstration of all the techniques discussed is demonstrated. The final chapter discusses about the conclusion along with future work. It describes about three possible directions in which this work can be extended.

2. DMD DEVICE-ITS ARCHITECTURE AND CAPABILITIES

In this chapter the development of a new type of thermo graphic experiment is presented. The experimental setup is described in detail. This apparatus can be used for the conventional thermography techniques at micro scale using laser as heat source, as well as significantly demonstrating the feasibility to identify cracks and thermal property distinction for system identification using spatial temporal modulation experiments.

2.1 DMD DEVICE

Digital Micro mirror Device (DMD) was developed by Texas Instruments in 1987 as a part of digital light processing device [24] .This patented technology used to manipulate the light at finer scale to project with higher resolution. It is used almost in 85% of the digital cinema projection and used to manipulate the power sources for additive manufacturing. A DMD chip consists of thousands of individually addressable aluminum mirrors each of which can be steered. This is an example of a commercially successful Micro-Electro-Mechanical System (MEMS). One such individual micro mirror architecture is shown in Figure. 2.1. The aluminum mirror is mounted on using a yoke present in the electric field. It is a comparable technology with Liquid Crystal Display (LCD) to project light in TV, Projectors etc. Although both have their own range of advantages, for this experiment DMD is considered suitable.
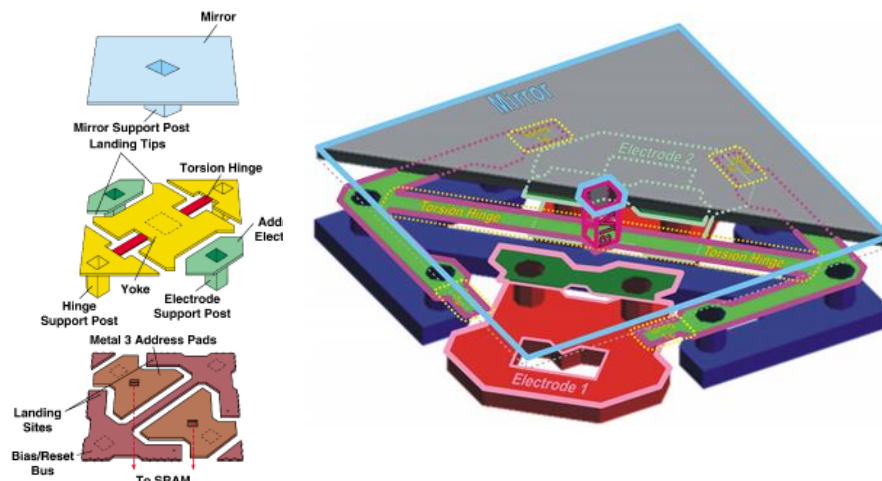
Figure.2.1 Micro mirror architecture present in DMD[24, 25]

The experiments in this thesis use a DLP 0.55 XGA chipset. This is a 0.55 in. diagonal micro mirror array, with 10.8µm Micro mirror pitch [26] having 1024 x 768 pixels. Each mirror can deflect either -12 or +12°, with the -12°off the axis is considered OFF and +12° off the axis is considered ON. The ON state projects the light at the desired output location, whereas OFF state projects it on the heat sink to dissipate the power. A compact cooling system with heat sink mounting along with radial fan is present, as the maximum temperature it can withstand is between 80˚C to 90˚C. Since, the mirrors are articulated under the electric field, they can be modulated as high as 80 kHz digitally. The mirror which is capable of flipping to ON and OFF states at such frequencies can produce 1024 shades of grey. This different shades of grey is synchronized with the color wheel to produce the appropriate color of the input image. But, as for this experiment is concerned, the color wheel is redundant and is isolated from the circuit. This range enables the experimenter to manipulate the laser beam either to direct it towards the sample or towards a sink. When a single micro mirror is modulated at a specific frequency, the laser beam is modulated at the same frequency of the mirror. When the consecutive mirrors are manipulated in a series, the laser beam is rastered over the surface. This enables to perform spatial thermo reflectance. Both spatial and temporal modulation is possible when the mirrors are manipulated simultaneously at specific frequencies.

The CMOS Substrate receives the signal and manipulates the movement of micro mirror. The projected light is collimated back to the sample surface using conventional optics. The negative of the image is focused to the sink to absorb the remaining radiation. The temperature variation due to periodic heat source is observed through uncooled micro bolometer thermal camera. The data is recorded and processed in the computer through MATLAB. Figure 2.2 illustrates the dimension of the Micro mirror Array through SEM image taken at 500X.
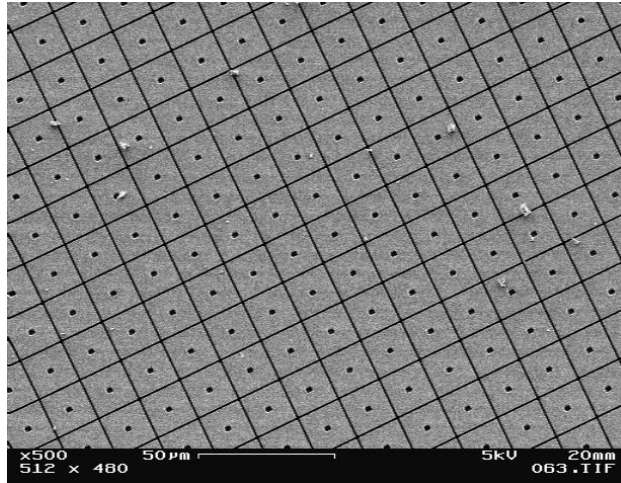
Figure.2.2 SEM image of the Micro mirror Array[27]

2.2 EXPERIMENTAL SET UP.

The simplified experimental setup is shown in Figure.2.3 and is described in a 3D Block diagram in Figure. 2.4. The heat source utilized in this experiment is a Coherent DUO-FAP Diode Laser of 800 nm and 532nm wavelength with maximum power of 30W each. Only one of the two outputs is used for this experiment. The diode output is transmitted through a fiber optic cable which is collimated over the DMD module of the Projector assembly. The DMD assembly is extracted from DELL 1409X Projector for convenience. One of the lighter objectives of the experiment is to make the system robust and cheap. In order to accomplish it, a hack was made in an old unused projector which had burnt out lamp. The micro mirrors in the DMD are controlled via MATLAB through a video output from the CPU. MATLAB code is used to generate videos of geometries varying periodically at specific frequencies and is given at Appendix. These videos are played in CPU and are passed on to DMD via VGA 15-pin connector cable. Figure.2.3 shows the Experimental set-up inside the shielded enclosure. The detailed block diagram is illustrated in Figure. 2.4.
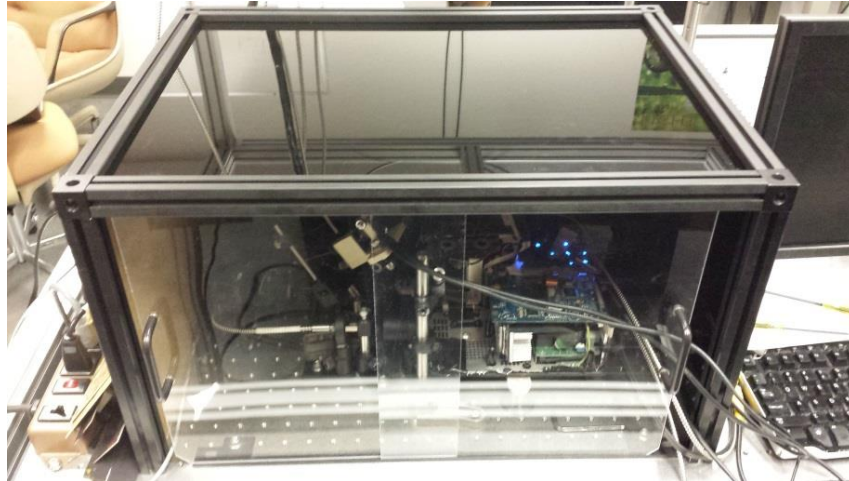
Figure.2.3 Experimental set up inside the shielded enclosure
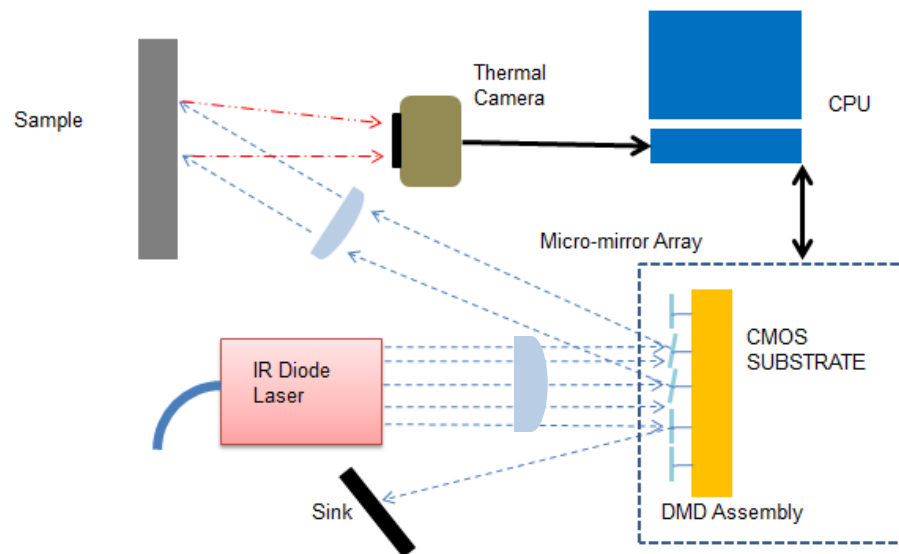
Figure.2.4 Experimental setup where laser is collimated over the DMD array

2.3 CAPABILITIES OF THE DEVICE:

The device is capable of performing (i) Pulse, (ii) Lockin, thermography (iii) spatial and temporal modulated thermography

2.3.1 Pulse Thermography. Pulse thermography as discussed earlier is a short emission of laser radiation or heat flux on the sample. The short pulse is absorbed by the surface, locally heating the first few micrometers. The thermal energy diffuses through the sample via conduction and the surface begins to cool. In regions where the conductivity is substantially different than the host media (e.g. an abscess, crack, or buried metal trace) the conduction away from the surface is disrupted, which affects the surface temperature. Deviations in the surface temperature can be observed with a thermal camera and used to identify and locate defects in the sample. Usually in conventional pulse thermography, the whole sample is pulsed with the flash lamp heat source [2, 5, 21]. The flash lamps provide huge radiative heat flux and are cheaper compared to laser source. In this work, the laser is used as it is a coherent, continuous wave heat source which is directional with minimum loss. It is highly desired for the spatial temporal modulation of the heat source, where precise control of heat flux is necessary. Since, the location, shape and size of the defect are generally not known a priority, it often takes multiple experiments to identify and qualitatively characterize a defect [28].

With the help of DMD device, simultaneous pulsing can be done and also pulsing of different flux density is possible by varying the area of the laser beam being projected. It is illustrated in the Figure.2.5. The diameter of the pulse can be precisely controlled by the DMD with the help of image generated by MATLAB.
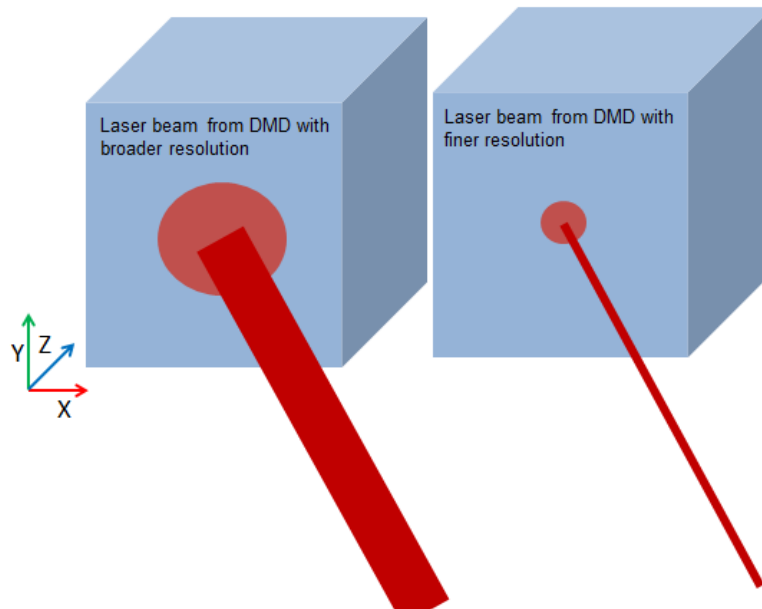
Figure.2.5 Sample is pulsed at different diameter by the DMD Device

2.3.2   Lock-in Thermography. Lock-in thermography as mentioned earlier is gives more quantification of the defect compared to the pulse thermography. But, the conventional setup[19, 22] is expensive utilizing high end signal processing tools. The signal processing is indeed necessary to increase the noise filtering capabilities, but with the help of fast Fourier transform the image is processed in simple fashion at the lock in frequency. In conventional setup in order to identify and characterize several lock in frequencies need to be done sequentially and is a time consuming process[28]. Using the DMD device, the pattern projected can be controlled based on the need and can perform simultaneous lock in thermography which are discrete in spatial domain.

Figure.2.6 illustrates the use of the device to simultaneously lock in at multiple frequencies as well as the possibility to lock-in with different profile. This is highly useful in identifying cracks and performing localized lock in thermography in structures like Wind Turbines or Aerospace structures where the whole sample cannot be illuminated by the flash lamp for lock in thermography. Even when illuminated, it will be insensitive to finer cracks. The pattern projected can be optimized for identifying the defects in quicker fashion. It is a control and optimization problem by itself and is beyond the scope of this work.

When lock in at different frequency is done, there is possibility of pulse compression where the phase match of the neighboring heat wave occurs and forms a pulse[29].
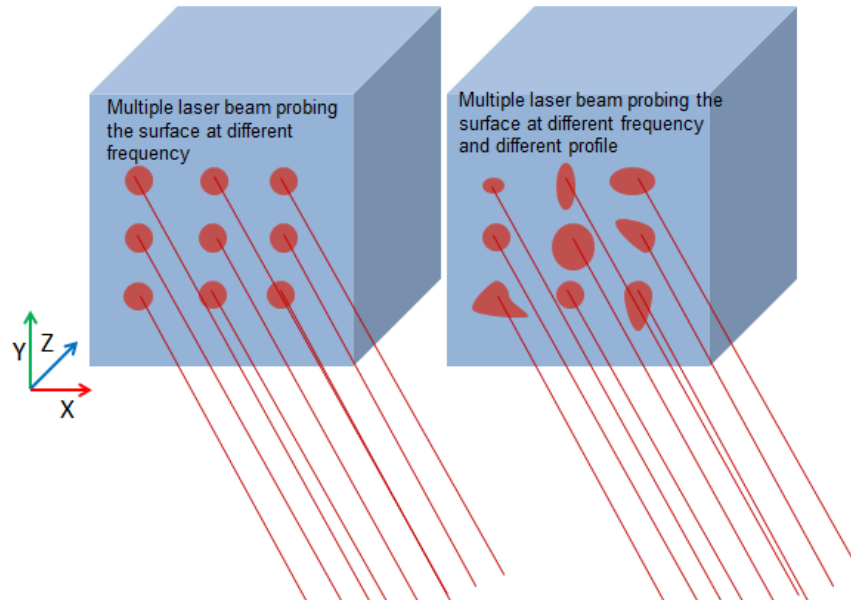
Figure.2.6 Sample is pulsed at different frequency and profile by DMD Device

2.3.3   Spatial and Temporal Modulation Thermography. Scanning the laser beam is highly useful technique to identify the cracks or defects in XY plane. As the laser beam is probed over the surface, the discontinuity acts as a non-conducting medium preventing the heat transfer along XY plane. This creates a heat spot and can be highly useful for quick evaluation of the defect. This defect is difficult to evaluate using conventional pulse or lock-in thermography. Comparing the conventional pulse, lock in thermography techniques this requires a different set up and is usually done with the help of laser beam[30].

The DMD device developed in this work is robust to perform the scanning laser beam technique to identify the defects in the cross plane as shown in Figure.2.7. The moving laser beam is manipulated by the movie created using MATLAB. The location, the rate of scanning and the diameter of the profile is controlled precisely by MATLAB.

Instead of just one spatially modulated beam, the beam can be temporally modulated to be immune from the DC noise affecting the signal. The spatially and temporally modulated beam has higher sensitivity to crack which is not detected under conventional flash or lock-in thermography[31]. For a larger area, multiple point or line heat source can be modulated spatially and temporally to identify the crack. The signal from the whole surface is locked in at all the corresponding lock-in frequency.
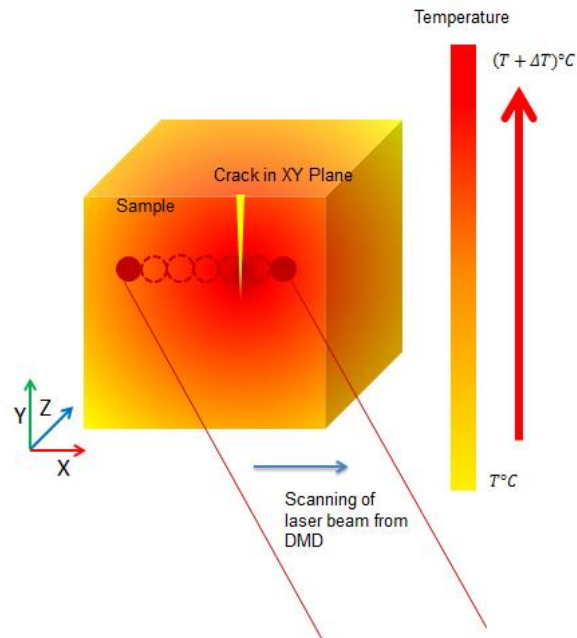
Figure.2.7 Sample is probed by scanning laser beam by DMD Device
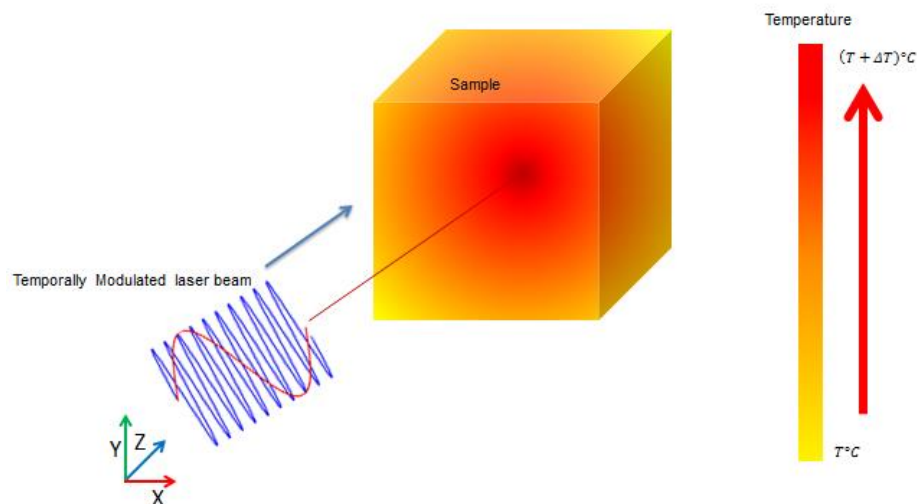
Figure.2.8 Temporal Modulation by DMD Device by different frequencies

2.4 LINEAR CO-ORDINATE TRANSFORMATION

The co-ordinate linear transformation is a mathematical tool to map the desired set from one plane to the other[32]. In this experiment, the camera which is parallel to the plane of the sample would observe a skewed image from the DMD projector. For the ease of analysis, a proper geometry would be helpful. In order to facilitate it, the linear transformation is used to find the skewed image which can project a proper geometry on the plane of the sample. It is shown in Figure.2.9 and the general equation of the transformation is shown in Eq.8. In this equation, transformation T maps the geometry from (u,v) plane to (x,y) plane.

$$T\ (u,\ v) = \big(x\ (u,v),y\ (u,\ v)\big) \tag{8}$$
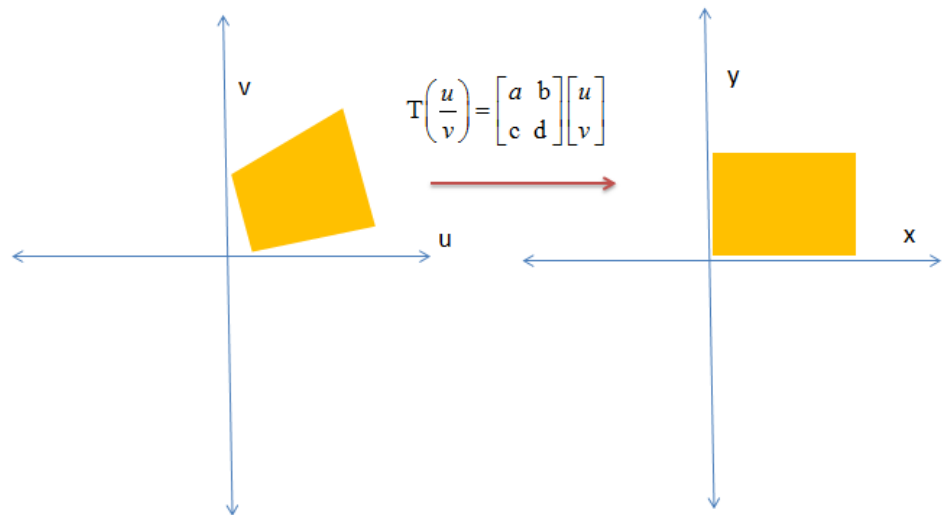
Figure.2.9 Linear Co-ordinate transformation mapping from the computer to the sample

The following is a detailed mathematical description of the process. In this experiment, there are two planes under discussion. One is the plane in the computer graphics which controls the DMD, the other is the projected image plane. For ease, the earlier one is called control plane and the other one is called projected plane. The co-ordinate points of the rectangle in control plane are namely (x_1 , y_1),(x_2 , y_2),(x_3 , y_3) and (

x_4, y_4) as shown in Figure.2.10. Similarly, the points in the projected plane are called (i_1, j_1),(i_2, j_2),(i_3, j_3) and (i_4, j_4).
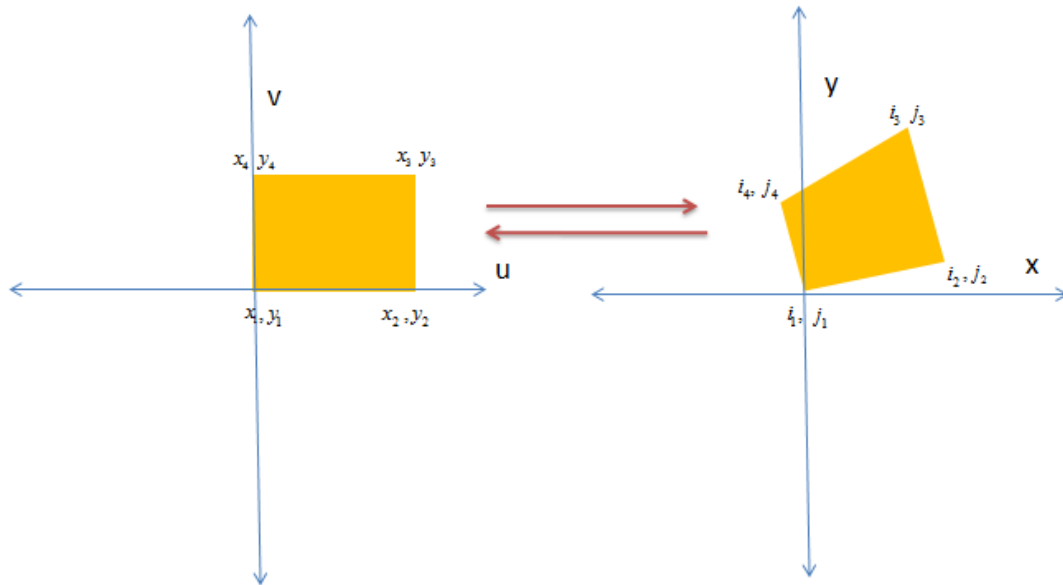
Figure.2.10. Mapping of co-ordinates between different planes

The simple transform equation for first point would be:

$$\begin{bmatrix} a & b \\ c & d \end{bmatrix}\begin{bmatrix} x_1 \\ y_1 \end{bmatrix} = \begin{bmatrix} i_1 \\ j_1 \end{bmatrix}$$

(9)

Similarly, there are three more set of linear equations.

$$\begin{bmatrix} a & b \\ c & d \end{bmatrix}\begin{bmatrix} x_2 \\ y_2 \end{bmatrix} = \begin{bmatrix} i_2 \\ j_2 \end{bmatrix}$$

(10)

$$\begin{bmatrix} a & b \\ c & d \end{bmatrix}\begin{bmatrix} x_3 \\ y_3 \end{bmatrix} = \begin{bmatrix} i_3 \\ j_3 \end{bmatrix}$$

(11)

$$\begin{bmatrix} a & b \\ c & d \end{bmatrix}\begin{bmatrix} x_4 \\ y_4 \end{bmatrix} = \begin{bmatrix} i_4 \\ j_4 \end{bmatrix}$$

(12)

Solving any of these four simultaneous equations the constants a, b, c, d can be found.

The co-ordinates of the desired geometry which needs to be projected in the projected plane are already known as it is the desired parameter. In this case, let those co-ordinates be $(i_1', j_1'), (i_2', j_2'), (i_3', j_3')$ and (i_4', j_4') respectively. Using the transformation constants a, b, c, d and the new desired control points (x_1', y_1') can be found. It is shown in Eq. (13). Likewise the other new co-ordinates can be found

$$\cdot \begin{bmatrix} x_1' \\ y_1' \end{bmatrix} = \begin{bmatrix} i_1' \\ j_1' \end{bmatrix} \begin{bmatrix} a & b \\ c & d \end{bmatrix}^{-1} \tag{13}$$

3. NUMERICAL ANALYSIS

In this chapter, the details of the numerical model are explained. Transient thermal problems are always complex and unpredictable. This complexity is one of the key obstacles in understanding the heat transfer propagation in the material which evolves in space and time. As direct analytical models are even more complex to capture all the dynamics and boundary conditions, numerical models are preferred to be used. Numerical model helps to understand the physics behind the experiment and enables to foresee the results. It also enables us to perform parametric and optimization studies beforehand.

In order to perform, numerical analysis Finite Element Method (FEM) is used. FEM is one of the most popular numerical techniques to perform transient heat transfer simulations. It has the versatility to handle material non linearity and nonlinear boundary conditions. ANSYS Workbench is used for this project as it is one of the well-established FEM solver used to perform multi-physics simulations.

The experiment verifies the numerical model and the explanation for any offset behaviors are explained.

3.1 GOVERNING EQUATION

The experiment involves all the three forms of heat transfer like Conduction, Convection and Radiation. Radiation is considered negligible or has been accommodated in the model if found to have reasonable contribution. The model generated is a 2-D approximation numerical model where Z<<(X, Y). So the conduction along XY plane is high compared to YZ plane.

Equation (3) is the heat conduction diffusion equation derived from Fourier law of heat conduction where the heat diffusion along x, y, z is represented. For pulse thermography, Equation (14) & (15) are applied to the elements where the heat pulse is applied. For the elements where no heat is applied Equation(16) is applied.

$$\frac{\partial T}{\partial t} = \alpha \nabla^2 T \tag{4}$$

Where $\nabla = \left(\dfrac{\partial}{\partial x} + \dfrac{\partial}{\partial y} + \dfrac{\partial}{\partial z} \right)$

When $time \in [0, time_{pulse}]$

$$k\left(\frac{\partial T}{\partial x} + \frac{\partial T}{\partial y} + \frac{\partial T}{\partial z} \right) = -q_0 + h_{conv}(T - T_{amb}) + \sigma\varepsilon(T^4 - T_{amb}^4) \tag{14}$$

When $time \in [time_{pulse}, time_{end}]$

$$k\left(\frac{\partial T}{\partial x} + \frac{\partial T}{\partial y} + \frac{\partial T}{\partial z} \right) = h_{conv}(T - T_{amb}) + \sigma\varepsilon(T^4 - T_{amb}^4) \tag{15}$$

The elements where heat is not applied, $time \in [0, time_{end}]$

$$k\left(\frac{\partial T}{\partial x} + \frac{\partial T}{\partial y} + \frac{\partial T}{\partial z} \right) = h_{conv}(T - T_{amb}) + \sigma\varepsilon(T^4 - T_{amb}^4) \tag{16}$$

For lock-in thermography, the input heat q_0 in Equation (14) is modified to periodic function as shown in Equation (17), where Q is the peak power during the period. The element where the heat is applied is similar to pulse thermography.

$$q = \frac{Q}{2}(1 + \cos(\omega t)) \tag{17}$$

The temperature distribution for periodic heat source is already discussed with the help of Equation (5) and (6) under lock-in thermography section.

$$T(0,t) = Ti + \Delta T \sin(\omega t) \tag{5}$$

$$\frac{T(x,t) - Ti}{\Delta T} = e^{(-x\sqrt{\omega/2\alpha})} Sin(\omega t - x\sqrt{\omega/2\alpha}) \tag{6}$$

$\alpha = k/(\rho * C_p)$, and $\omega = 2\pi\nu$

3.2 BOUNDARY CONDITION

The model has three types of boundary conditions: Firstly, Heat flux with convection and radiation, Secondly, Convection with constant temperature Thirdly, Convection with radiation. The heat flux with convection is applied on the top surface where the laser beam is projected. From experiment, the Heat flux is measured to be within the range of 500 to 1000W/m^2. Convection boundary condition is implied on all the 18 faces of the sample which includes the surface area covered by the defects. Convection co-efficient of 10 W/m^2.$^{\circ}$C is applied along these faces subjected to standard atmospheric temperature and pressure. Second type of boundary condition is applied on the base of the model, to simulate real time conditions. All other sides have third type of boundary condition. Radiation is applied if the sample under investigation has high emissivity. The samples are either black in color or are subjected to a black coat to maximize the absorptivity. This is would just influence the amplitude of the signal and is insensitive to phase.

3.3 FINITE ELEMENT MODELING

3.3.1. Geometric Modeling. In order to simulate the physics, 2D approximation of the sample is created to reduce computational time and for straight forward description of the results. Geometric modeling is performed using the Design Modeler in the ANSYS Workbench 14. The dimension of the sample is shown in Figure.3.1. The design has been parametrized for future optimization. The named selection has been created to apply load and boundary condition as shown in Figure.3.2.
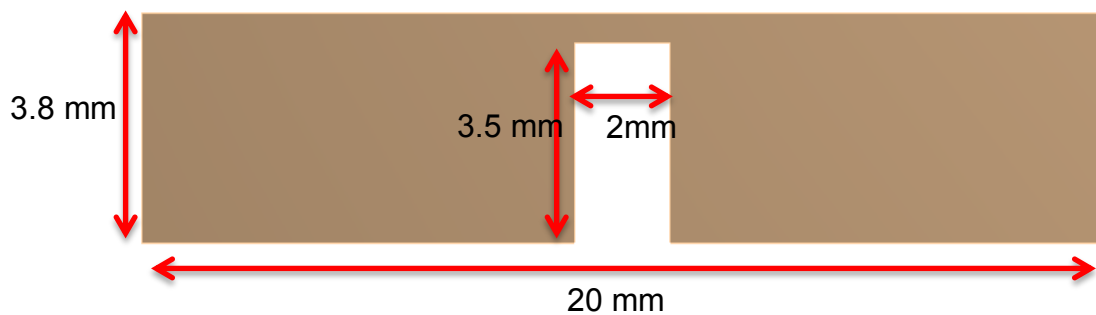
Figure.3.1 Dimension of the sample as made in Design Modeler of Ansys Workbench 14.

Named Selection- To define the segment where laser beam can be applied
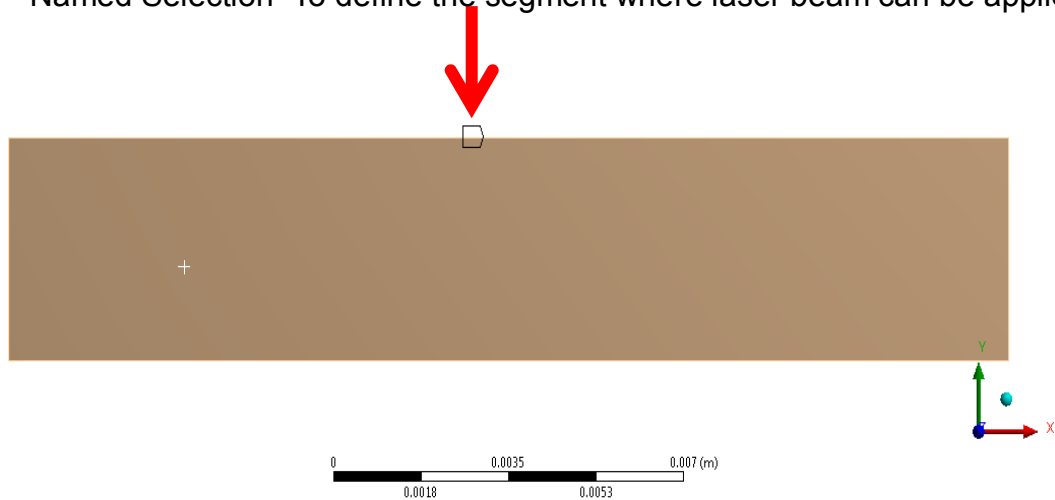
Figure.3.2 Named Selection in the geometric modeling to specify Thermal load

3.3.2. Meshing. The next immediate process in the finite element modeling procedure is to define the mesh volumes. So the geometry is sub divided into smaller finite volumes. Tetrahedron mesh is applied to the body and finer refinement is applied in the places of defects where changes in temperature are of primary interest. The mesh with edge refinement is shown in Figure.3.3 and the setting is shown in Figure.3.4.

Edge Refinement in the Area of Interest
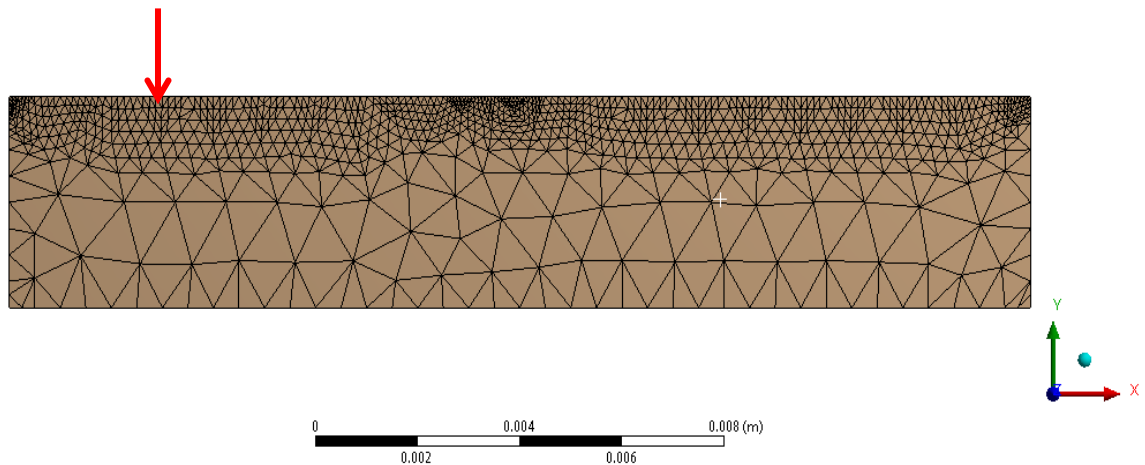
Figure.3.3 Tetrahedron Mesh with fine refinement on the area of interest

Sizing

Use Advanced Size Fun...	Off
Relevance Center	Coarse
☐ Element Size	Default
Initial Size Seed	Active Assembly
Smoothing	Medium
Transition	Fast
Span Angle Center	Coarse
Minimum Edge Length	1.e-004 m

Figure.3.4. Mesh Setting

3.3.2. Solution and Post Processing. The solution setting decides the accuracy of the solution. For pulse thermography the solution solver setting is shown as in Table.3.1. For Lock-in Thermography solution solver setting is shown as in Table.3.2. The results and post processing are discussed in the Results chapter.

Table 3.1. Solution Setting for Pulse Thermography

Time	Time Step
0 - 0.05	0.00001
0.05 - 0.1	0.0001
0.1 - 1	0.001
1 - 15	0.01
15 - 50	0.1

Table 3.2. Solution Setting for Lock-in Thermography

Time	Time Step
0-15	.01

4. RESULTS

This chapter is split up into two sections. First section discusses the numerical results which describes the existence of the problem and predicts the solution to the problem statement. The later discusses about the experimental results. The experimental results consist of conventional pulse, lock in thermography, material property estimation for system identification, crack detection using spatial temporal modulation and application of simultaneous spatial temporal modulation.

4.1 NUMERICAL RESULTS

In this section, 2-D approximated Numerical models have been simulated and the results are discussed. The numerical simulation of conventional pulse thermography, lock-in thermography and spatial temporal modulation for crack identification are discussed. The simulation helps in understanding the physics of the problem and possible solution. The material property used in this model is FR-4.The thermal property used for the numerical simulation is shown in Table.4.1.

Table.4.1 Properties of FR-4 used in the simulation

Thermal Property	Value, units
Thermal Conductivity in W/m.K	0.294
Density in kg/m^3	1900
Specific heat capacity, kJ/kg.K	1150

4.1.1. Pulse Thermography. In the pulse thermography, the whole surface under inspection is flashed with the uniform heat flux. In figure. 4.1 the following numerical result shows the heat propagation when uniform heat flux is applied over the surface. The crack of 2mm of 20mm length FR-4 beam is easily detectable using pulse thermography. As the camera used in the experiment is based on the gradient in temperature, the temperature scale is redundant information. The use of un-calibrated camera is one of the key advantage and power of this technique.

When the same heat flux is applied over the sample which has a fine crack of 0.1mm, the temperature gradient is insensitive and it is extremely difficult to see any temperature gradient. This is seen in the Figure. 4.2.
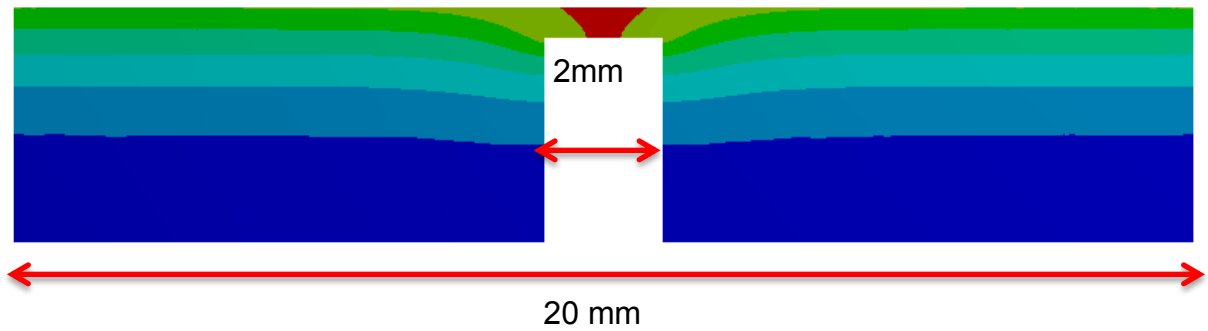
Figure.4.1 Pulse Thermography on wide defect
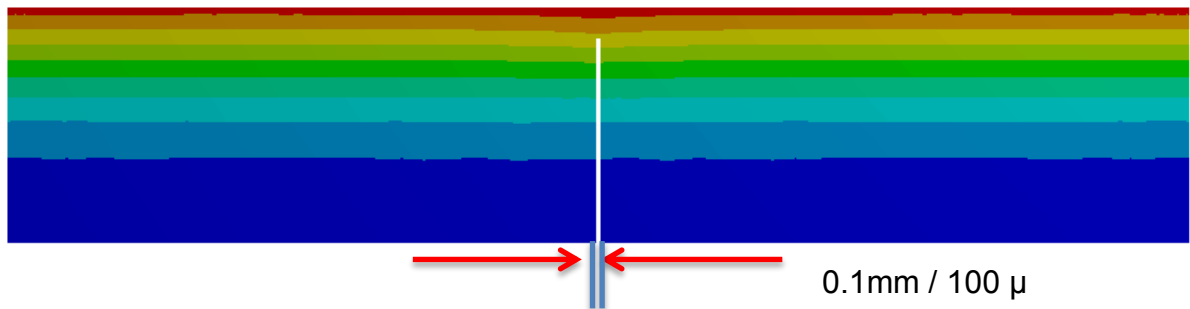
Figure.4.2 Pulse Thermography on narrow defect

4.1.2. Lock-in Thermography. In lock in thermography, the heat source is varied periodically at specific frequency. The frequency depends on the thermal penetration depth required, which is discussed in earlier chapters. The lock-in thermography also can identify the defect present at 0.35 mm beneath the surface present in FR-4 using a lock-in frequency of 350 mHz, which is shown in Figure. 4.3. But, a challenge arises when the same frequency is applied to the sample with defect at the same depth but with narrower width. As seen in the Figure. 4.4 the conventional lock-in frequency is not able to identify the crack defect. The method is insensitive to fine cracks which are less than 1% of the area under exposure.

Figure.4.3 Lock-in Thermography on wide defect
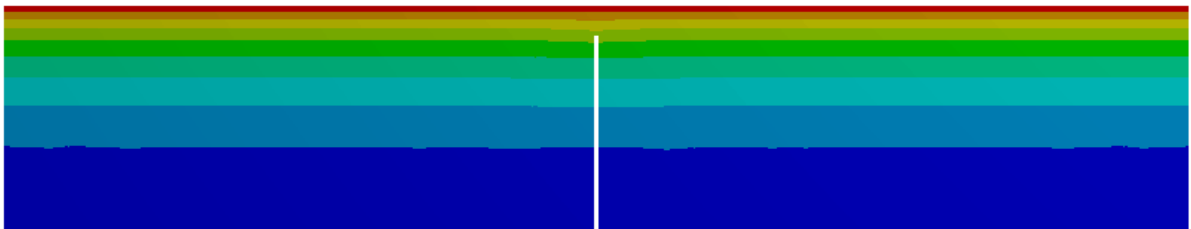
Figure.4.4 Lock-in Thermography on narrow defect

4.1.3. Spatial and Temporal Modulated Thermography. In spatial and temporal modulation lock-in thermography the crack can be identified by using the same amount of heat flux but having the heat source applied at the localized zone where the conduction of thermal waves is hindered by the narrow crack. This perturbation is seen as a discontinuity in the thermal contrast. In pulse thermography, it is sensitive to discontinuity and temperature contrast can be seen. In lock-in the thermography the discontinuity is seen both in amplitude and phase maps. This is demonstrated as shown in Figure.4.5 and Figure.4.6 for pulse and lock-in thermography respectively.
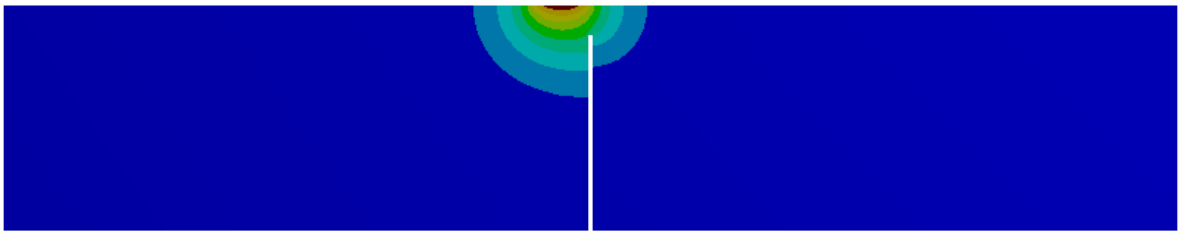
Figure.4.5 Spatially modulated Pulse Thermography
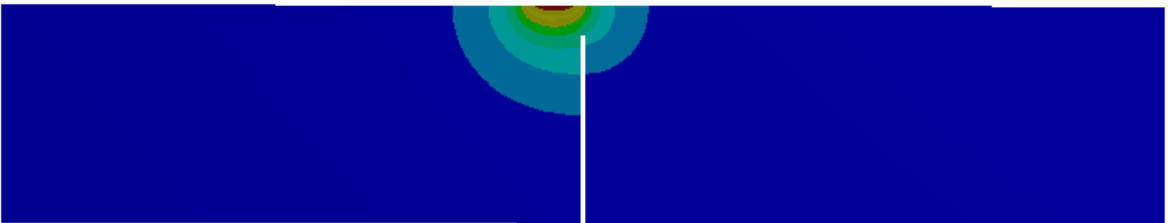
Figure.4.6.Spatially and Temporally modulated Lock-in Thermography

4.2 EXPERIMENTAL RESULTS

Experiments have been performed demonstrating conventional pulse thermography, lock-in thermography, crack-detection and finally the capability to perform multiple spatial and temporal thermography.

4.2.1. Pulse Thermography. In pulse thermography, a sample made up of ABS plastic has been used. Heat flux of 2.68 W/inch^2 (4166W/m^2) has been applied. The defect at a depth of 0.635 mm has been inspected. The picture shows the initial heating phase for 15 seconds and cooling for 35 seconds. The temperature profile of healthy segment and defective segment are shown in the Figure.4.7.
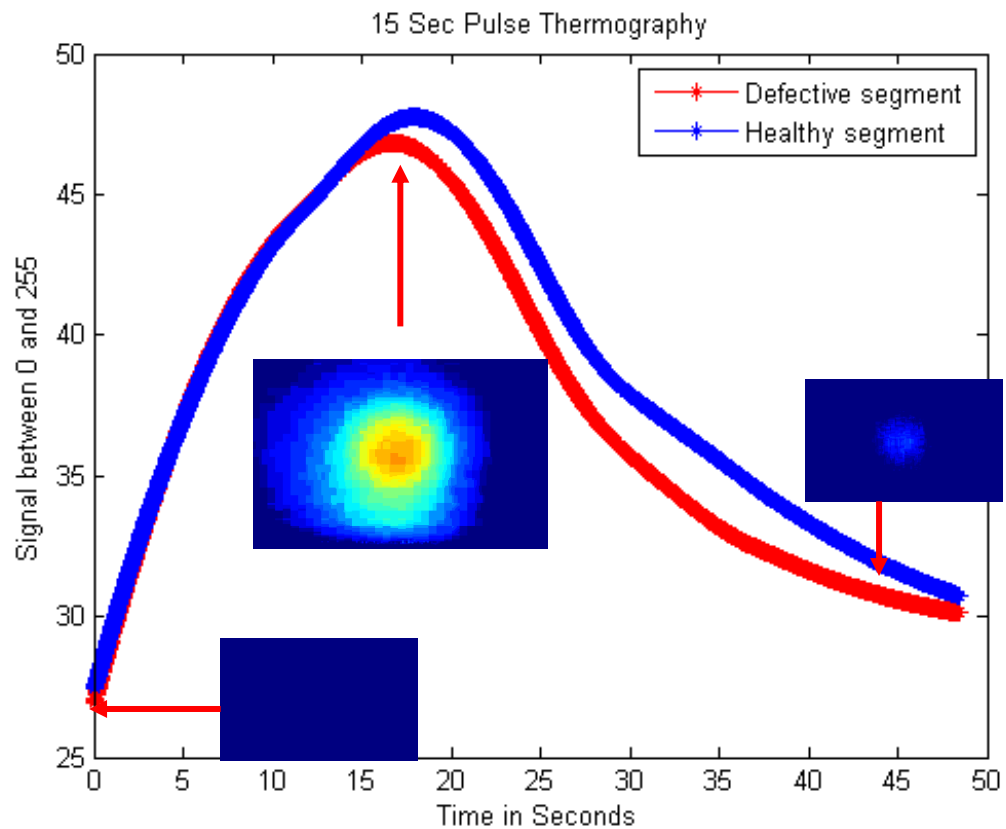
Figure.4.7 15 sec Pulse Thermography

4.2.2. Lock-in Thermography. In lock-in thermography the defect of 2.54mm diameter at a depth of 0.635mm is used to demonstrate the lock-in thermography capability. Although a uniform heat flux is applied, the heat conduction is hindered in the defective area and gets accumulated resulting in temperature rise. This is reflected in the amplitude and phase map. After performing FFT of the signal, the amplitude and phase map at 97.5 mHz is illustrated as shown in Figure.4.8. The temperature variation at the location 1,2 and 3 is shown in the Figure.4.8. The decrease in amplitude and marginal shift in phase can be seen in Figure4.9 due to the presence of defect. The FFT of the thermal wave is plotted on the right in Figure.4.9.
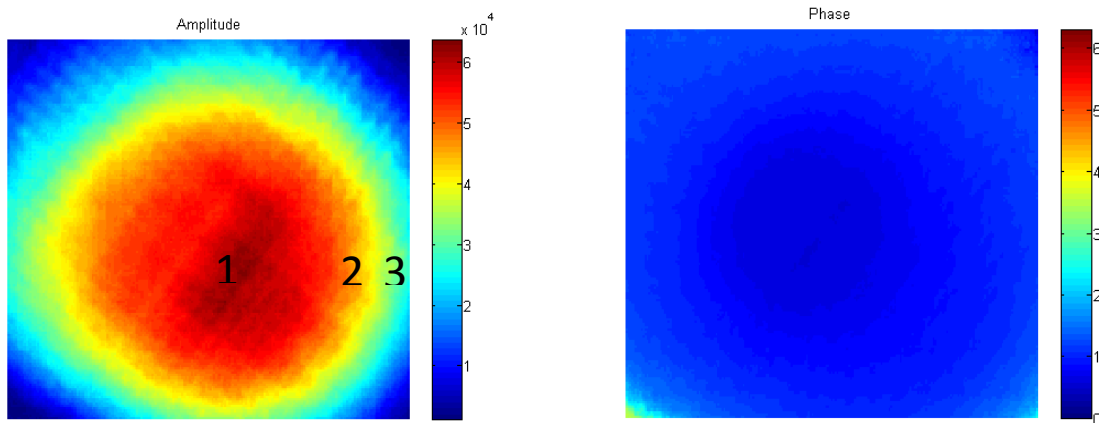
Figure.4.8 Amplitude and Phase image of the defective ABS sample
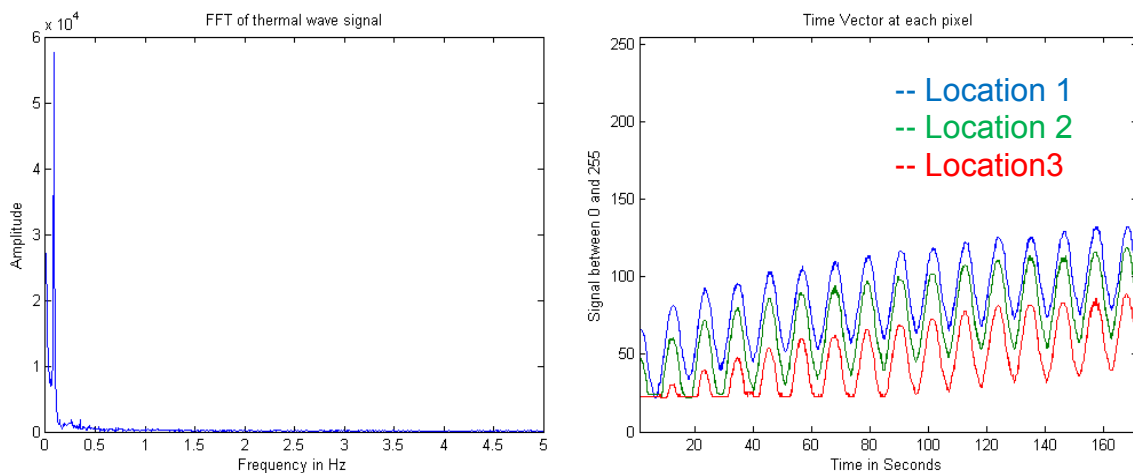
Figure.4.9 FFT plot and the location of defects as shown in Figure.4.8

4.2.3. Crack Identification. In order to find a fine crack, a spatially modulated beam is required as seen from Figure.4.5 and Figure.4.6. As temporally modulated heat source is more advantageous in terms of noise filtering and eliminating DC components. Hence, a spatial and temporally modulated laser beam is used to identify the cracks.
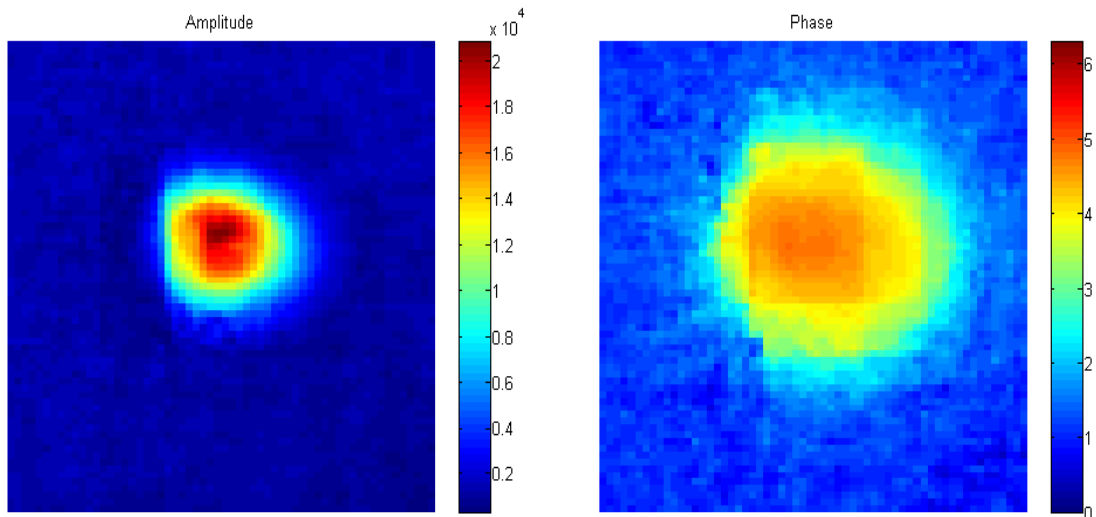
Figure.4.10 Amplitude and Phase map of spatially and temporally modulated heat source

The crack is simulated using two glass slides having extremely smooth surface finish. This crack is roughly between 50-100µ. The amplitude and phase map is shown in Figure.4.10.The laser beam diameter is 1.5mm which can be seen from the Figure.4.11. The glass slide is coated black in order absorb and utilize maximum amount of radiation. The laser beam is modulated at 100mHz. The amplitude and phase plot are sensitive to the crack and is illustrated in Figure. 4.11. The amplitude plot is exactly sensitive to the crack compared to phase. This phenomenon can be attributed to the conduction across the crack for such low frequency. A higher frequency could yield more sensitivity in phase. But the sensitivity analysis is a study by itself and requires computational guidance.
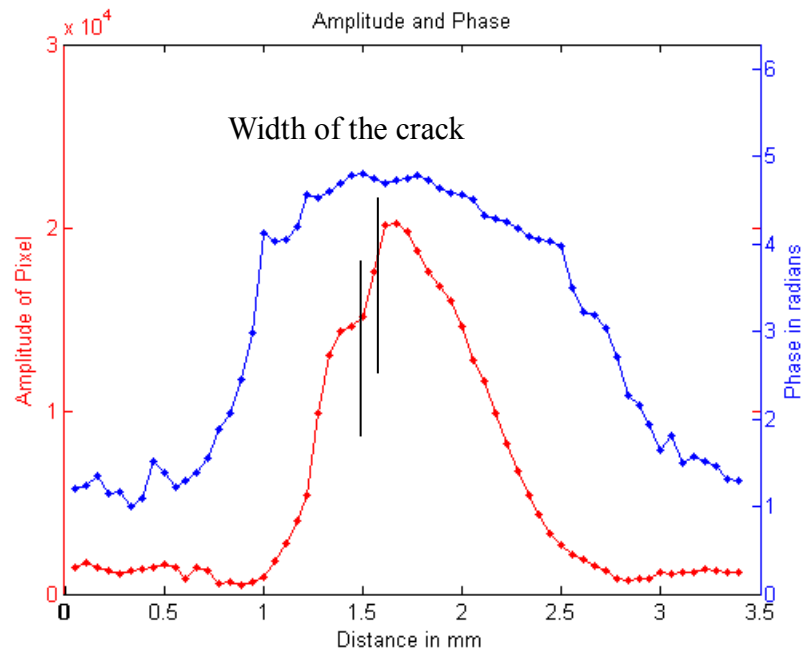
Figure.4.11 Amplitude and Phase segment transverse to the crack

4.2.4. Multiple Spatial and Temporal Modulations. As discussed in the previous section, the identification of crack requires a localized spatial temporal modulation. This is a cumbersome process to follow when the area under scanning is of higher order in magnitude compared to the crack. Unfortunately, the reality is that the cracks are always going to be finer and be several orders lower from the actual dimension of the sample. In order to perform the search for cracks multiple spatial temporal modulation is required. This is enabled with the help of DMD and is demonstrated by having two line heat sources being periodic and spatially apart from each other. One line of 1Hz and other with 2Hz is pulsing periodically on the cu-cladding of FR-4 surface. The raw and the processed image on color scale are illustrated in Figure.4.12.
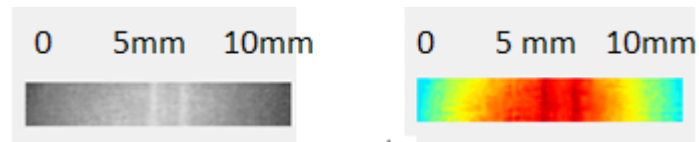
Figure.4.12 Segment of Raw signal from the DRS camera and the corresponding color image
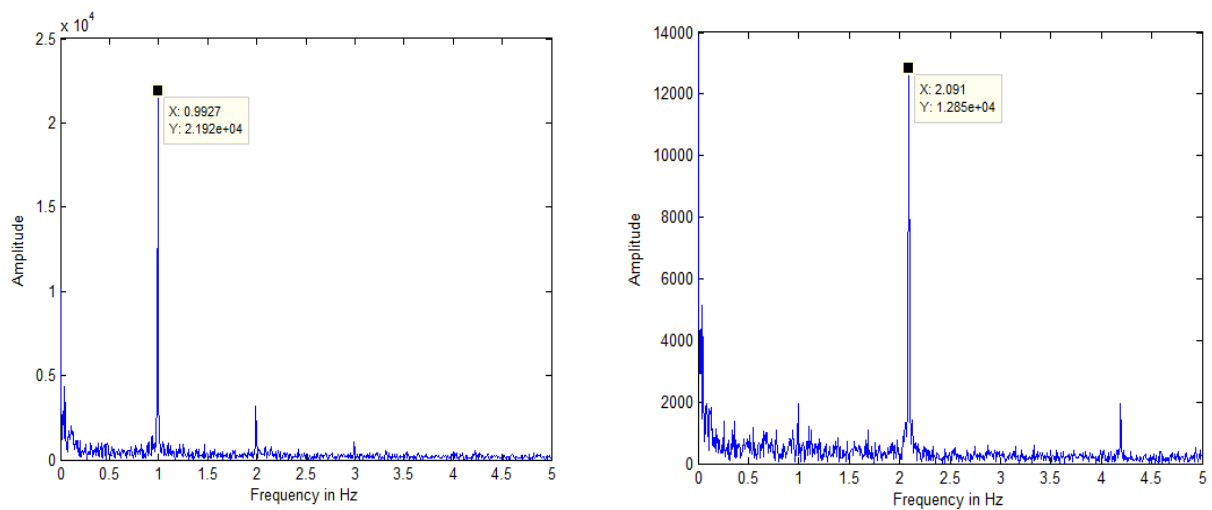
Figure.4.13.FFT plot of each line
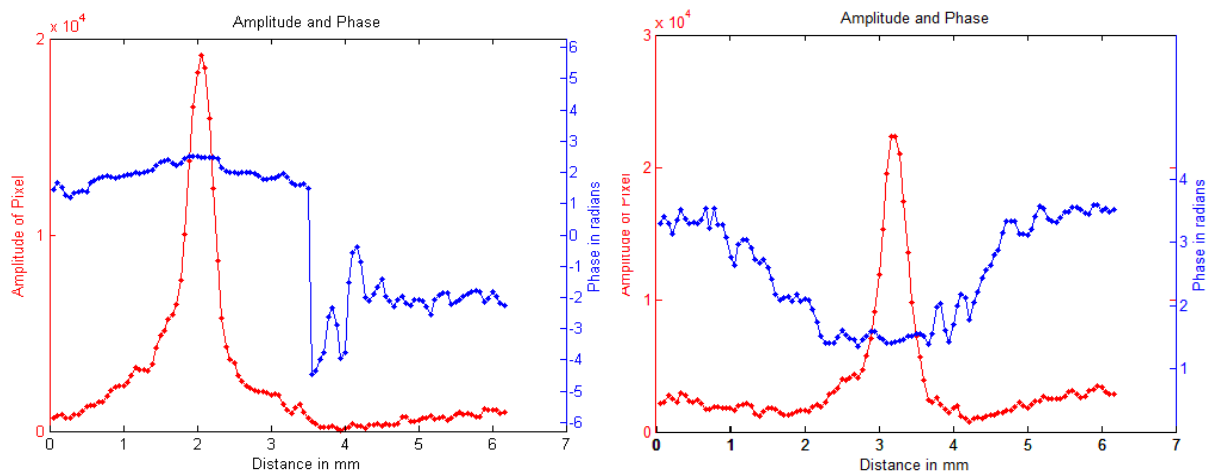
Figure.4.14.Amplitude and Phase plot corresponding to 1Hz and 2Hz

4.2.5. Thermal Property Estimation for System Identification. Thermal property estimation is highly useful for system identification purposes. The following experiment is conducted on FR-4 with copper cladding of 35μm. The objective of the experiment is to distinguish the FR-4 surface from the copper cladding surface. The sample is coated black to enhance the radiation absorptivity. In order to analyze, a fine line heat source is modulated using the DMD at 600 mHz. The slope of phase roll is different for different materials and is a function of thermal diffusivity,α. In Figure.4.15 the amplitude and phase image of the line heat source modulated at 600 mHz over FR-4 is illustrated and the corresponding FFT plot along with segment plot of amplitude and phase is illustrated in Figure.4.16. Likewise the line heat source modulated at 600 mHz over copper cladding is illustrated in Figure.4.17 and the corresponding segmented plots along with FFT is illustrated in Figure. 4.18. From the slope of the phase from the location of the heat source, it can be easily identified that a metal surface is present or absent even for very fine thickness like 35μm. The slope of the phase is close to flat as the in-plane conductivity of the cu-clad is higher compared to through plane conduction.
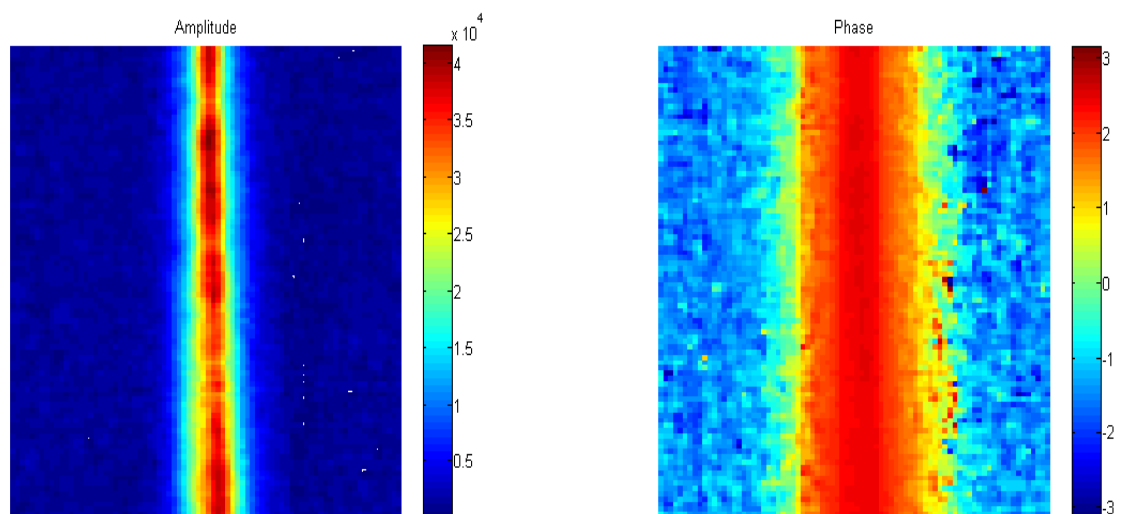
Figure.4.15.Amplitude and Phase plot corresponding of 600mHz shining at FR-4 surface
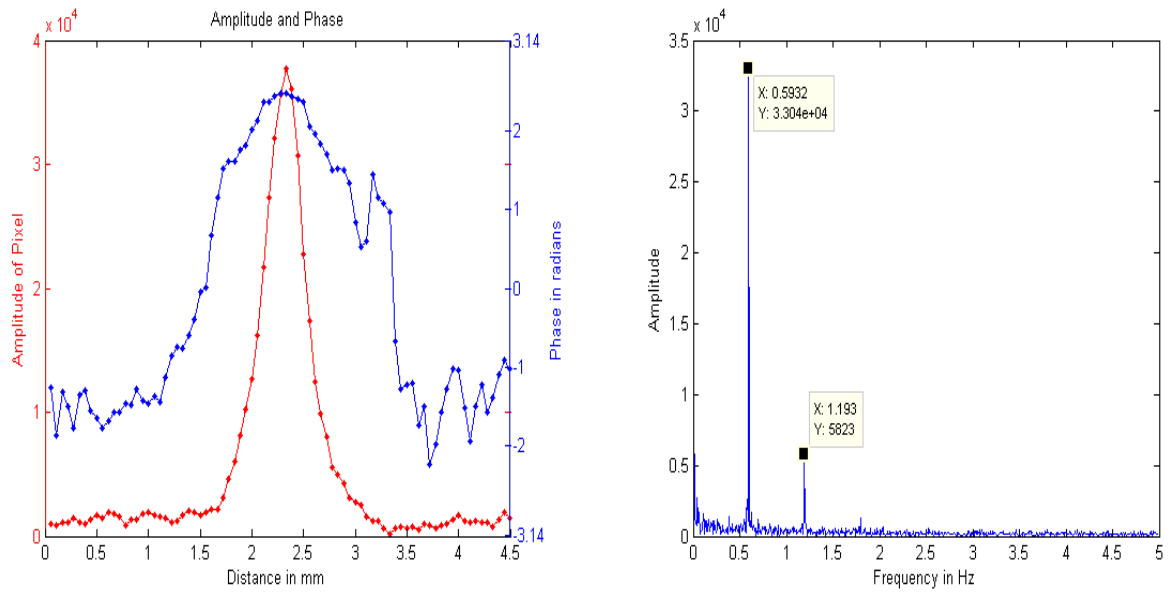
Figure.4.16.Amplitude and Phase plot on FR-4 (on Left) along with FFT plot (on Right)
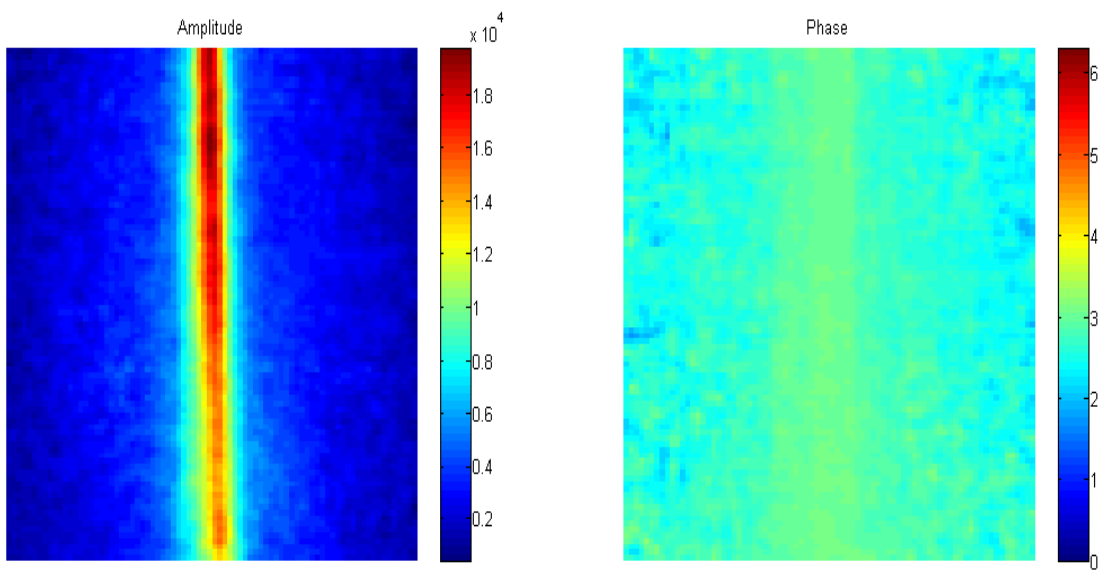
Figure.4.17. Amplitude and Phase plot corresponding to 600mHz shining at copper-cladding surface
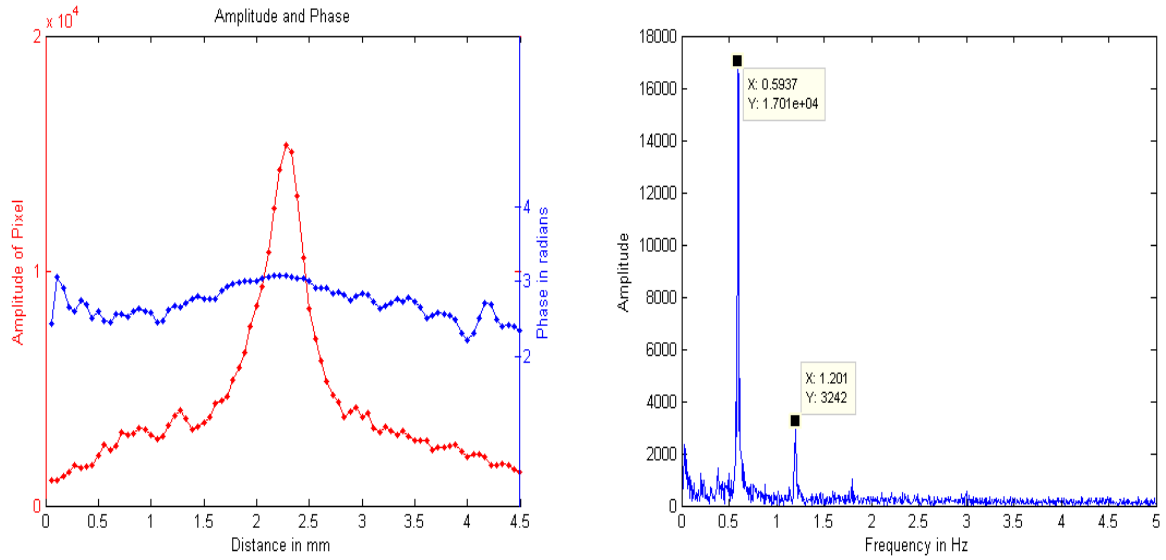
Figure.4.18.Amplitude and Phase plot on Copper cladding (on Left) along with FFT plot (on Right)

5. CONCLUSION AND FUTURE WORK

5.1 CONCLUSION

Non-Destructive Testing (NDT) is highly essential in improving the confidence in quality of the products. With humongous product lines in today's industry there is a need to perform simultaneous NDT techniques. The device built in this work enables to work towards that goal. The instrument's capability to perform (i) Pulse thermography, (ii) Lock-in thermography (iii) spatially and temporally modulated thermography were demonstrated. The need to quantify the defect using advancement in thermography was realized and a device was fabricated in that direction. The capability of the device was established. The application of these principles to future work is discussed as under.

5.2. FUTURE WORK

The future work is really interesting as plenty of opportunities are ahead. The future work is broadly classified under three directions. Firstly, based on the thermography technique for crack detection, Secondly, based on system identification using the thermal property distinction, Thirdly, based on the application of the system to diverse areas in order to solve commercial challenges.

5.2.1 Direction-1. In order to search the cracks in the sample a parametric optimization is needed to identify the optimal parameters which are sensitive to fine cracks. The variables are as shown in Figure.5.1, frequency of the heat source 'f', the laser spot diameter 'a', the distance away from the crack 'b' for a specific crack width 'd' and specific crack height 'c'. This whole sensitivity analysis could vary for different thermal diffusivity as different materials have different thermal time constant.

The real time search of the crack can be a classical optimal control problem. The state variable would be the phase of the temperature profile at the surface and the control variable would be the frequency of the laser beam along with the spot diameter. The cost function of the problem can be defined as the time to search the cracks and with a feedback of the state variable identifying the discontinuity in amplitude and phase of the map. The schematic is illustrated in Figure.5.2.
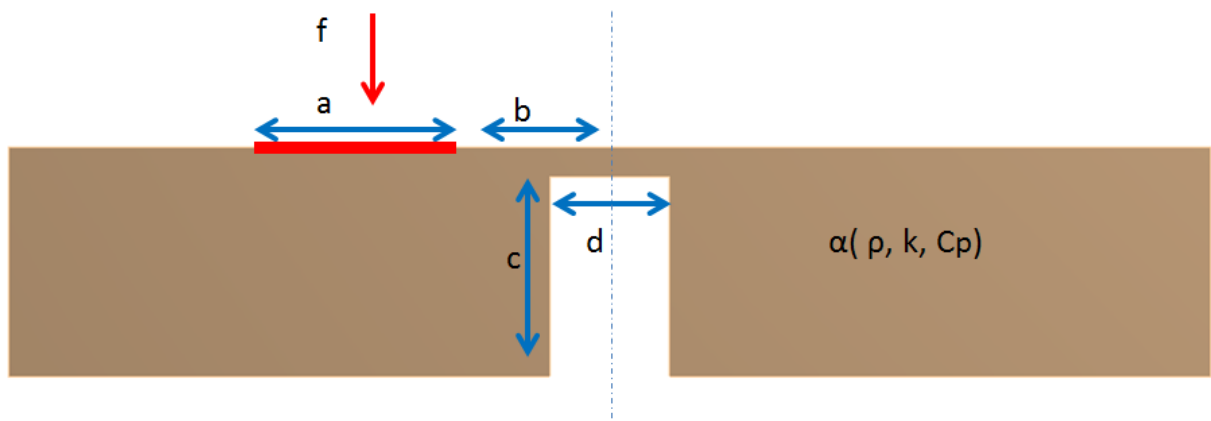
Figure. 5.1 Parametric Optimization and Control theory
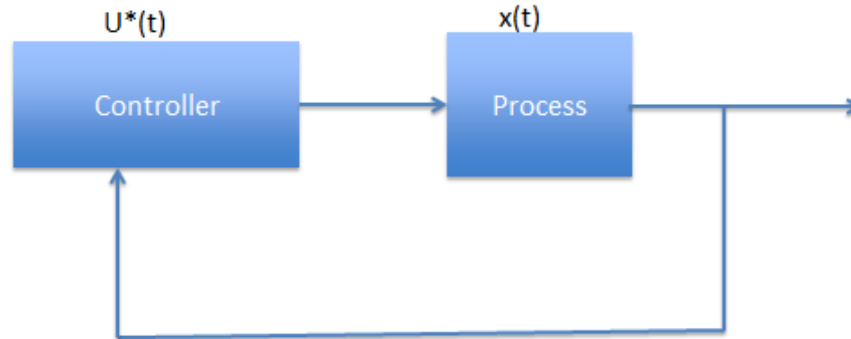
Figure. 5.2 Feedback based Closed Loop Optimal Control Problem

5.2.2 Direction-2. The current technique is useful in identifying and distinguishing materials based on the thermal properties. The value addition to the technique would be generating 3-D profile of the geometry along with the thermal data imbibed in them for better understanding of the sample. The sample can be scanned by projecting optical fringes using similar DMD light modulator and the scattered distorted light can be captured using two simultaneous CCD cameras placed at known perspective from the sample. Thus, the captured light could be reconstructed to form 3D image as shown in Fig.5.3. As the lockin technique is insensitive to orientation and illumination, the thermal property information along the surface could be imbibed to the 3D model.

Figure.5.3 Structured light 3D scanner scanning a car seat to generate 3-D profile [33]

5.2.3 Direction-3. The third direction would be to apply the technique in solving challenges of commercial interests. One great application for different commercial problems:

Deploying in autonomous mobile systems to identify obstacles while performing rescue operations. Deploying in system with a conveyor system to identify cracks and defects demonstrating for industries like electronics industry(Find cracks in circuits, defects in soldering or printing of circuits), fuel cell industry (To detect cracks in graphite plates which are expensive during pre and post manufacturing conditions).

Currently, the DMD used in the experiment can handle only a maximum of 50W. It can be enhanced by arranging multiple DMDs to cover a larger area and the search for cracks in large samples would be feasible. Also fine resolution of DMD can provide higher resolution of thermal projections which can improve the sensitivity.

APPENDIX

To control the experiment, multiple MATLAB codes were written. These codes perform the following tasks:

A. To control the laser
B. To generate videos of specific frequency or pattern to manipulate the DMD
C. To post process Lock-in Thermography video
D. To post process Pulse Thermography video
E. To post process the amplitude and phase result to create GIF movie

MATLAB CODES TO CONTROL LASER

In order to communicate with the laser an 'object' has to be created and string values needs to be passed on to them.

The following code creates an object called 'laser' to which string values can be passed on. The user can change the port to COM1 or COM2 depending on the availability. The string '0**1**o1' controls laser 1 and string '0**2**o1' controls laser 2. This is applicable for all similar commands where the appropriate laser needs to be addressed.

%%%START%%%

```
laser = instrfind('Type', 'serial', 'Port', 'COM3', 'Tag', '');
if isempty(laser)
    laser = serial('COM3');
else
    fclose(laser);
    laser = laser(1);
end
set(laser, 'Terminator', [1]);
set(laser, 'Timeout', 5.0);
fopen(laser);
```


%%%

Laser Status Control

%%%START%%%

```
fprintf(laser,'01o0');  % Switch OFF
fprintf(laser,'01o1');  % Switch ON and Get Ready
fprintf(laser,'01o2');   % Active and Fire
```

%%%END%%%

The following is the code to control the laser to vary the power periodically for specific frequency.

The first part of the code creates the sine wave form and the second part uses the data to manipulate the power according to the data. The waveform generated is passed on to the laser as string. A minute pause is created for the hardware to respond. This will have negligible effect, as the maximum frequency in this experiment is 15Hz due to nyquist limitation.

% First Part%

%%%START%%%


```
Fs=30;% Sampling rate (Lower sampling rate for lower frequency and higher sampling
rate for higher frequency)
fz=0.5;% Frequency of the signal
dt=1/Fs;
TotalTime=10;
t=(0:dt:TotalTime-dt);
x=2500+1500*sin(2*pi*fz*t);  % Defining the range of power
y=int32(x); % Converting to Integer
figure
plot(t,x,'-*')
xlabel('Time in Seconds');
title('Wave');
[~,n]=size(y);

% Second part
fprintf(laser, '01o0');
fprintf(laser, '01o1');
pause(2)
fprintf(laser,'01o2');
for i=1:n
    k=num2str(y(1,i));
    fprintf(laser,'01p0[;%s]\r',k);
    pause(.00005)
end
fprintf(laser, '01o1');
```

%%%END%%%

MATLAB CODE TO GENERATE VIDEOS TO MANIPULATE DMD

Create a line scan video for scanning laser beam thermography

The following code enables to create a vertical line and move it. This video is generated to scan the surface with the laser beam. The user has control of the rate at which the line can move, the length of the line and the overall size of the plot area, the thickness of the line. The sampling rate helps in controlling the rate at which the line can move, the 'LineWidth' helps in controlling the thickness of the line.

%%%START%%%

```
writerObj = VideoWriter('output.avi');
open(writerObj);
x1=(1:.25:50);
x2=(1:.25:50);
y1=1;
y2=100;
[~,no]=size(x1);
for i=1:no
    drawnow
    plot([x1(i),x2(i)],[y1,y2],'Color','black','LineWidth',6)
    set(gca,'XLim',[0 50], 'YLim',[0 100]);
    set(gca, 'xtick', [], 'ytick', []) ;
    set(gcf,'color','w');
    set(gca, 'xcolor', 'w', 'ycolor', 'w');
    drawnow
    frame = getframe(1);
    writeVideo(writerObj,frame);
end
close(writerObj);
```

%%%

The following code enables to create a horizontal line and move it. This video is generated to scan the surface with the laser beam. It is similar to the code above.

%%%START%%%

```
clear
writerObj = VideoWriter('output.avi');
open(writerObj);
x1=1;
x2=100;
y1=(1:.25:100);
y2=(1:.25:100);
```

```
[~,no]=size(y1);
for i=1:no
    drawnow
    plot([x1,x2],[y1(i),y2(i)],'Color','black','LineWidth',6)
    set(gca,'XLim',[0 100], 'YLim',[0 100]);
    set(gca, 'xtick', [], 'ytick', []) ;
    set(gcf,'color','w');
    set(gca, 'xcolor', 'w', 'ycolor', 'w');
    drawnow
    frame = getframe(1);
    writeVideo(writerObj,frame);
end
```

%%%END%%%

To create a video with moving spot to raster the laser beam from top to bottom. Co-ordinates in the XY plane, the radius of the spot can be controlled.

%%%START%%%

```
clc;
clear;
writerObj = VideoWriter('A1.avi');
open(writerObj);
rows =480;%Creates the matrix grid
cols = 720;
r1 = 25;
y=1:3:cols;
x=150;
[~,no]=size(y);
  % In [X,Y] coordinates
[xMat,yMat] = meshgrid(1:cols,1:rows);
for i=1:no
  center1 = [x y(i)];
  distFromCenter1 = sqrt((xMat-center1(1)).^2 + (yMat-center1(2)).^2);
  circleMat1 = distFromCenter1<=r1;
  I1=(mat2gray(~circleMat1));
  set(gcf,'color','w');
  imshow(I1);
  drawnow
  frame = getframe(1);
  writeVideo(writerObj,frame);
end
close(writerObj);
```

%%%END%%%

To create a video with moving spot to raster the laser beam along a rectangle oriented along the diagonal of the screen. Co-ordinates in the XY plane, the radius of the spot can be controlled.

%%%START%%%

```
clc;
clear;
writerObj = VideoWriter('output.avi');
open(writerObj);
rows =720;
cols = 720;
r1 = 45;
t=(-720:15:720);
x=abs(80-t);
y=abs(t)+20;
[~,no]=size(x);
 [xMat,yMat] = meshgrid(1:cols,1:rows);
for i=1:no
  center1 = [x(i) y(i)];
  distFromCenter1 = sqrt((xMat-center1(1)).^2 + (yMat-center1(2)).^2);
  circleMat1 = distFromCenter1<=r1;
  I1=(mat2gray(~circleMat1));
  set(gcf,'color','w');
  imshow(I1);
  drawnow
  frame = getframe(1);
  writeVideo(writerObj,frame);
end
close(writerObj);
```

%%%END%%%

 To create a video circular spot that will vary its intensity in a periodic fashion. In this, the control of frequency, the intensity (0 to 255), the phase (0 to 2π) is possible.

%%%START%%%

```
clear;
clc;
rows =240;
cols = 240;
r1 = 25;%Radius of the spot
center1 = [64 128];  % In [X,Y] coordinates
```

```
% Make the circle
[xMat,yMat] = meshgrid(1:cols,1:rows);
distFromCenter1 = sqrt((xMat-center1(1)).^2 + (yMat-center1(2)).^2);
circleMat1 = distFromCenter1<=r1;
I2=(mat2gray(~circleMat2));
writerObj = VideoWriter('output.avi');
open(writerObj);

Fs=25; % Sampling
fz1=1;% Frequency
phi1=0; % Phase (It might be useful to control phase when multiple spots are generated)
dt =1/Fs;
TotalTime=240;
t=(0:dt:TotalTime-dt);
x1=2500+2500*sin((2*pi*fz2*t)+phi2);
xi=[x1/max(x1)];
[~,ni]=size (t);
for n=1:ni
NI=xi(:,n)+I2;
imshow(NI);
set(gcf,'color','w');
frame = getframe(1);
writeVideo(writerObj,frame);
end
close(writerObj);

%%%END%%%
```

MATLAB CODE TO POST-PROCESS THERMAL VIDEOS FROM LOCK-IN THERMOGRAPHY

The following code helps to find the lock-in frequency from the video. Spot1 is the pixel which is of interest. The pixel of interest can be seen by having **implay**(output_video). Or The 3D matrix which is squeezed from the movie. The original video would be a 4D matrix and can be squeezed to 3D. The extra dimension present in the video represents the color scale of the video. In case of thermal camera videos it would pass on the information as greyscale. So the index '1' will be truncated and made into 3D matrix by using the squeeze command.

```
%%%START%%%

spot1=squeeze(v1(23,23,:)); % Pick a pixel in the area of interest and apply
pit=spot1;
fp=fft(pit);%FFT of the time signal
phase=angle(fp); % Phase
dp=abs(fp);   % Amplitude
```

```
[r,~]=size(pit);
frate=30;
f = frate/r*(0:(2*round((0.5*r)/2)-1));
[~,sf]=size(f);
dp5=dp(1:2*(round(0.5*r/2))+1);
dp5(1,:)=[];%Removing high amplitude DC
figure
plot([f(:,1:sf/3)],dp5(1:sf/3,1),'-b')
xlabel('Frequency in Hz');
ylabel('Amplitude');
title('FFT of thermal wave signal');
set(gcf,'color','w');

%%%END%%%
```

The following is the code to perform Lock-in thermography using all the pixels in the Input_video:

```
%%%START%%%

clear
vido=VideoReader('Input_Video.wmv'); % Input your .avi or .wmv file here
v=read(vido);
v1=squeeze(v(1:190,:,1,:));% Convert the 4-D matrix to 3-D matrix
nc1=imresize(v4,1);% If the matrix needs to be resized for computational purposes(quick
result, %poor resolution)
[p q r]=size(nc1);k2=[];
%Creating the time vector of individual pixel
for i=1:p
    for j=1:q
        k=nc1(i,j,:);
        k2=[k2,k];
         end
end
% %
phs=zeros(p*q,round(0.5*r));nmag=zeros(p*q,round(0.5*r));
f = 30/r*(0:(2*round((0.5*r)/2)-1));
%% Below is the FFT process, where FFT of the time vector in each pixel is done.
Amplitude %and phase are calculated
for i=1:p*q
    fast=(fft(k2(1,i,:)));
    fast(1)=[];
    fnew=fast(1:(length(fast)/2)+1);
    sigphase = angle(fnew);
    phs(i,:)=sigphase;
```

```
    mag = abs(fnew);
    nmag(i,:)=mag;
end
k2=[];
fz=1; % Plug-in the exact lock-in frequency for accurate results
[~, yin] = min(abs(f - fz));
yi=[1:(p*q)];
nmat1=[];nmat2=[];
magblk=nmag(:,yin);phblk=phs(:,yin);newphase=[];

% For manipulating phase between –π and π
for i=1:p*q
    newphase(i,:)=phblk(i,1);

end


 % For manipulating phase between 0 to 2π
for i=1:p*q
    if phblk(i,1)>0
        remin=rem(phblk(i,1),2*pi);
        r1=remin;
    else
        pd2=phblk(i,1)+1000*pi;
        r1=rem(pd2,2*pi);
    end
        newphase(i,:)=r1;
end
 %

for  i=1:(q):((p*q)-(q-1))
    nmat=magblk(i:(i+(q-1)));
    nmat1=[nmat1;nmat'];
    phmat=newphase(i:(i+(q-1)));
    nmat2=[nmat2;phmat'];
end
% %  Plots
figure
h1=surf(nmat1);
title('Amplitude')
axis([1 q 1 p])
view(2)
set(gcf,'color','w');
set(gca,'YDir','reverse');
set(gca,'XTick',[]);
set(gca,'YTick',[]);
```

```
colorbar
grid off
set(h1,'edgecolor','none');
figure
h2=surf(nmat2);
title('Phase')
axis([1 q 1 p])
view(2)
set(gcf,'color','w');
set(gca,'YDir','reverse');
set(gca,'XTick',[]);
set(gca,'YTick',[]);
set(h2,'edgecolor','none');
% caxis([-pi pi]),colorbar  %  Should be used if the phase is between −π and π
caxis([0 2*pi]),colorbar
grid off

%%%END%%%


Line plot from Amplitude and Phase surface plot

%%%START%%%

figure
 [~,ps]=size(nmat1);
% [ps,~]=size(nmat1); Depends on the orientation of the line
mm=(1:ps)./18; %1mm=18pixel(Measure the Field of View)
pnt=30;
 [haxes,hline1,hline2] = plotyy(((mm)),nmat1(pnt,:),((mm)),nmat2(pnt,:));
set(hline1, 'LineStyle', '-','Marker', '.','Color',[1 0 0]);
set(hline2, 'LineStyle','-','Marker', '.','Color',[0 0 1]);
set(haxes(1),'YColor', [1 0 0]);
set(haxes(2),'YColor', [0 0 1]);
set(haxes(2),'YLim',[0 2*pi])
set(haxes(2),'YTick',[0 1 2 3 4 5 6])
% set(haxes(2),'YLim',[-pi pi])
% set(haxes(2),'YTick',[-3.14 -2 -1 0 1 2 3.14])
set(gcf,'color','w');
ylabel(haxes(1),'Amplitude of Pixel');
ylabel(haxes(2),'Phase in radians');
xlabel('Distance in mm');
title('Amplitude and Phase')

%%%END%%%
```

MATLAB CODE TO POST-PROCESS THERMAL VIDEOS FROM PULSE
THERMOGRAPHY

The pulse video is read and the pixel of interest is identified.
Then it is plotted.

```
%%%START%%%

clear;
clc;
% 15 Sec Pulse Thermography
vido=VideoReader('pulse15.wmv'); % Input your .wmv file here
v=read(vido);
v=squeeze(v(:,:,1,:));
v1=v(:,:,:);
[~,~,time]=size(v1);
ti=(1:time)./30;
% Identify the pixel locations in the area of interest and plug in aptly
D1=double(squeeze(v1(43,242,:)));
D3=double(squeeze(v1(45,95,:)));
D4=double(squeeze(v1(168,91,:)));
D2=double(squeeze(v1(162,242,:)));
D5=double(squeeze(v1(107,274,:)));
% D1=double(D1);
% The following smooth fitting function can be used to fit the raw data and obtain the
clean signal
y1 = smooth(ti,D1,0.5,'loess');
y2 = smooth(ti,D2,0.5,'loess');
y3 = smooth(ti,D3,0.5,'loess');
y4 = smooth(ti,D4,0.5,'loess');
y5 = smooth(ti,D5,0.5,'loess');

plot(ti,y1,'-*r',ti,y2,'-*b',ti,y3,'-*g',ti,y4,'-*y',ti,y5,'-*k')
title('15 Sec Pulse Thermography')
legend('2.54mm dia at 0.254mm','1.27mm dia at 0.254mm','2.54mm dia at
0.635mm','1.27mm dia at 0.635mm','Normal Sample')
xlabel('Time in Seconds');
ylabel('Signal between 0 and 255');
set(gcf,'color','w');

%%%END%%%
```

GIF MOVIE GENERATION FROM AMPLITUDE AND PHASE RESULT

This program uses the amplitude and phase data generated from the lock-in program

%%%START%%%

```
time=1:0.033:5; % Useful to control the time and time intreval
[~,tm]=size(time);
omega=2*pi*fz;
for i=1:tm
  shot=nmat1.*cos((nmat2)+omega*time(i));
  h3=surf(shot);
   set(gcf,'color','w');
  set(gca,'ZLim',[-30000 30000]);
  caxis([-30000 30000]);colorbar;
set(gca,'YDir','reverse');
 % view(2)     % (Turn ON if 2-D view is required)
  grid off
  axis off
  camlight;
   lighting phong
  set(gca, 'XTick', [], 'YTick',[]);
  set(h3,'edgecolor','none');
  mov(i) = getframe;
  [Inx,cmap]=rgb2ind(mov(i).cdata,256);
  if i==1
      imwrite(Inx,cmap,'output.gif','gif','DelayTime',0.3,'LoopCount',Inf)
  else
      imwrite(Inx,cmap,'output.gif','gif','WriteMode','append','DelayTime',0.3)
  end
end
```

%%%END%%%

BIBLIOGRAPHY

1.   Avdelidis, N. and D.P. Almond, *Transient thermography as a through skin imaging technique for aircraft assembly: modelling and experimental results.* Infrared physics & technology, 2004. 45(2): p. 103-114.

2.   Ducar, R.J. *Pulsed thermographic inspection and application in commercial aircraft repair.* in *AeroSense'99.* 1999. International Society for Optics and Photonics.

3.   Hellier, C. and C. Hellier, *Handbook of nondestructive evaluation.* Vol. 10. 2001: McGraw-Hill New York.

4.   Avdelidis, N., B. Hawtin, and D. Almond, *Transient thermography in the assessment of defects of aircraft composites.* NDT & E International, 2003. 36(6): p. 433-439.

5.   Genest, M., et al., *Pulsed thermography for non-destructive evaluation and damage growth monitoring of bonded repairs.* Composite Structures, 2009. 88(1): p. 112-120.

6.   Huth, S., et al., *Localization of gate oxide integrity defects in silicon metal-oxide-semiconductor structures with lock-in IR thermography.* Journal of Applied Physics, 2000. 88(7): p. 4000-4003.

7.   Liu, W. and B. Yang, *Thermography techniques for integrated circuits and semiconductor devices.* Sensor Review, 2007. 27(4): p. 298-309.

8. Quintard, V., et al., *Laser beam thermography of circuits in the particular case of passivated semiconductors.* Microelectronic Engineering, 1996. 31(1): p. 291-298.

9. Shpartko, P., et al., *Thermography in manufacturing: nondestructive evaluation of ultrasonic spot welds of automotive battery pack.* 11th Quantitative InfraRed Thermography. Naples, Italy, 2012.

10. Noethen, M., K.-J. Wolter, and N. Meyendorf. *Surface crack detection in ferritic and austenitic steel components using inductive heated thermography*. in *Electronics Technology (ISSE), 2010 33rd International Spring Seminar on*. 2010. IEEE.

11. Ley, O. and V. Godinez-Azcuaga, *Line Scanning Thermography and its Application Inspecting Aerospace Composites.*

12. YANG, Z.-W., W. ZHANG, and G. TIAN, *Numerical Simulation on Thermal Wave NDT of Missile Engine [J].* Nondestructive Testing, 2009. 1: p. 002.

13. Meola, C., et al., *The use of infrared thermography for nondestructive evaluation of joints.* Infrared physics & technology, 2004. 46(1): p. 93-99.

14. Zhou, Y. and M. Omar, *Dynamic-template processing for passive thermograms: Applied to automotive stamping split detection.* NDT & E International, 2008. 41(8): p. 582-588.

15. Lin, M., C. Ziqing, and W. Yuwen, *Pulse thermography analyzed by the finite element method for nondestructive testing.* Journal-Xian Jiaotong University, 2000. 34(1): p. 66-70.

16. Maldague, X. and S. Marinetti, *Pulse phase infrared thermography.* Journal of Applied Physics, 1996. 79(5): p. 2694-2698.

17. Shepard, S.M. *Advances in pulsed thermography*. in *Aerospace/Defense Sensing, Simulation, and Controls*. 2001. International Society for Optics and Photonics.

18. Bai, W. and B. Wong, *Evaluation of defects in composite plates under convective environments using lock-in thermography.* Measurement Science and Technology, 2001. 12(2): p. 142.

19. Breitenstein, O., W. Warta, and M. Langenkamp, *Lock-in thermography: Basics and use for evaluating electronic devices and materials*. Vol. 10. 2010: Springer.

20. Pickering, S. and D. Almond, *Matched excitation energy comparison of the pulse and lock-in thermography NDE techniques.* NDT & E International, 2008. 41(7): p. 501-509.

21. Sakagami, T. and S. Kubo, *Applications of pulse heating thermography and lock-in thermography to quantitative nondestructive evaluations.* Infrared Physics & Technology, 2002. 43(3): p. 211-218.

22. Wu, D. and G. Busse, *Lock-in thermography for nondestructive evaluation of materials.* Revue générale de thermique, 1998. 37(8): p. 693-703.

23. Carslaw, H.S., *Introduction to the mathematical theory of the conduction of heat in solids*. 1945, New York Dover Pub.

24. Lee, B. *Introduction to Digital Micromirror Device (DMD) Technology*. Revised October 2013; Application Report-DLPA008A–July 2008]. Available from: http://www.ti.com/lit/an/dlpa008a/dlpa008a.pdf.

25. *Architecture of the Texas Instruments Digital Micromirror Device (DMD).* [cited 2015; Available from: http://compliantmechanisms.byu.edu/content/introduction-microelectromechanical-systems-mems.

26. Instruments, T., *DLP 0.55 XGA Chipset.*

27. Jackson, J.D. *Visual Analysis of a Texas Instruments Digital Micromirror Device.* Available from: http://www.optics.rochester.edu/workgroups/cml/opt307/spr05/john/.

28. Chatterjee, K., et al., *A comparison of the pulsed, lock-in and frequency modulated thermography nondestructive evaluation techniques.* NDT & E International, 2011. 44(7): p. 655-667.

29. Tuli, S. and R. Mulaveesala, *Defect detection by pulse compression in frequency modulated thermal wave imaging.* Quantitative InfraRed Thermography Journal, 2005. 2(1): p. 41-54.

30. Li, T., D.P. Almond, and D.A.S. Rees, *Crack imaging by scanning pulsed laser spot thermography.* NDT & E International, 2011. 44(2): p. 216-225.

31. Pech-May, N., et al., *Vertical cracks characterization using lock-in thermography: I infinite cracks.* Measurement Science and Technology, 2014. 25(11): p. 115601.

32. Kreyszig, E., *Advanced engineering mathematics.* 1988: John Wiley & Sons.

33. *Structured-light_3D_scanner.* 2008 17:54, 18 March 2008 [cited 2015; Available from: http://en.wikipedia.org/wiki/Structured-light_3D_scanner.

VITA

Arvindvivek Ravichandran was born in Chennai, India. He was awarded Bachelors in Mechanical Engineering from Government College of Technology – Coimbatore under Anna University in 2008.

He has been working for four years as an engineer in Fuel Cell development and applications. He worked in Automotive Industry and National Lab in India. He enrolled in MS in Mechanical Engineering in Fall 2012 and has been awarded Teaching and Research Assistantship. He has been handling sections of Experimental Methods in Aerospace Engineering and Introduction to Design as Teaching Assistant. He was working in Thermal Radiation Laboratory as Research Assistant. He won Third Place in Student Infra-red Imaging Competition by DRS Technologies among the 27 teams from nationwide. He graduated with Masters in Mechanical Engineering in May 2015.